Spring 2018

Two Notes on a Piano

Samuel Thomas
swt6@zips.uakron.edu

Two Notes on a Piano

Samuel Thomas

Honors Research Project

Department of Physics

Abstract

In an increasingly digital world, the analog tends to be neglected in exchange for the convenience and precision of digital devices. However, many analog systems exhibit physical phenomena that can be difficult to reproduce digitally. The purpose of this project is to explore the piano and parts of its sonic character that are not currently accounted for in digital systems. Specifically, when multiple notes are being propagated on a soundboard, they affect each other's tone because each one changes the state of the soundboard. The effect is evident in the partials of each note: the partials (not quite harmonics but peaks in the power spectrum) will have the same frequencies but different power values. This changes the perception of the notes, the timbre. In digital devices, separately recorded notes are being summed as opposed to being played simultaneously on a piano, thereby losing this subtle change in timbre.

This work explores these two scenarios through computer simulations of a piano model. The model describes the soundboard, the strings, and the interaction between hammer and string. Using a finite difference method, we simulate the sound propagation of two notes being played separately and simultaneously. To investigate the effect of notes being played together, we determine power spectra for select locations on the soundboard and vibration patterns. To make the results relevant for real pianos within reasonable computational effort, we employ realistic parameters for materials and explore non-linear effects while maintaining a simplified soundboard geometry. Our results show measurable differences between the power spectra of two notes combined in the two scenarios (simultaneous and post-summed) and small non-linear effects.

Table of Contents

1 Introduction

I am a musician and a physicist and use a digital audio workstation to compose songs on my computer. Since I am also an audio engineer I have become rather sensitive to a lot of the technical, physical aspects of sound. My favorite virtual instrument is a program that does an excellent job of reproducing different types of pianos. It is sample based, which means it contains thousands of recorded piano sounds for every note, different striking velocities, different microphones in different locations, and probably more. The program takes commands from a midi controller to play these sounds, modified by the operator, in real time. It uses envelopes to control the attack, decay, sustain, and release times of the individual sounds to create a very real sounding virtual piano; it truly is a beautiful piece of software. However, because it is summing individually pre-recorded samples it lacks the nuance of a real, physical piano.

In his book, *Physics of the Piano* [1], Giordano discusses how, on a real piano, when notes are played simultaneously, they affect each other's tone because each one changes the state of the piano's soundboard. For instance, when a bass note is played, the mechanical impedance of the board changes, effectively changing the elastic characteristics of the board. When a second note is played on a board in this altered state, the effect is evident in the partials. For a musical tone, partials are peaks in the power spectrum at frequencies other than the note's fundamental but not necessarily at the frequencies of the higher harmonics. The spectrum of partials provides the timbre of the sound.

When a note is being played on soundboards in different states, we expect the partials to stay at the same frequencies but with potentially different magnitudes. This will change the timbre and, thus, the perception of the note's sound. I want to explore this effect of the physical system with the hope that it can one day be reproduced in the next great virtual instrument.

Computer simulations of piano models have provided insight into the generation of sounds by pianos. [2, 3, 4, 5] In earlier work, Ryan Bogucki and myself [6] developed programs to simulate sound propagation on a piano string struck by a hammer. These simulations were based on work by Chaigne and Askenfelt [2], [3] and on Giordano's *Computational Physics* [7]. The present work focuses on the role of the soundboard.

The principle of a piano is that a hammer strikes a string when triggered by a piano key. The hammer causes vibrations of the string, which are transferred to the piano's soundboard by way of a bridge. The vibrations of the soundboard generate the audible sound. The soundboard model used in this work is based on Giordano's papers [4, 5] and is simulated with a finite difference method. Figure 1 shows a sketch of the soundboard model and its components.

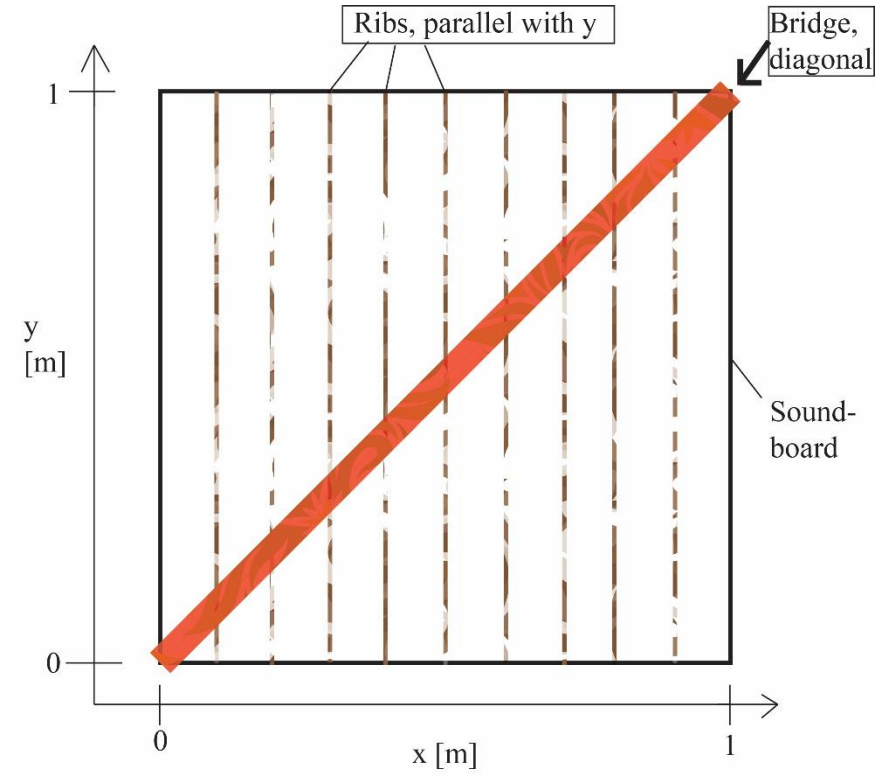

Figure 1: A sketch of the soundboard system and its components. The board lies, at rest, in the x-y plane. The keys of the piano would be at the location of the y-axis. The strings are parallel to the x-axis. The soundboard model describes three physical components, the soundboard, the ribs, and the bridge. The soundboard is a flat, square board of side length one meter and constant thickness. The ribs are attached to the bottom of the soundboard, parallel to the y-axis. The bridge sits on top of the soundboard and runs along the diagonal, $y = x$. The string force is applied at specific locations on the bridge. For instance, the string for the bass note B2 is on the left side of the keyboard, at y = 70 cm and its string force is applied at the x, y – coordinates (70 cm, 70 cm). In contrast, the string force for the higher note, A5, is applied at (34 cm, 34 cm). The diagonal orientation of the bridge is practical since the strings of the higher notes are shorter than those of the lower notes.

In order to investigate the idea of piano tones having different timbres if they are being played together on a piano (scenario I) as opposed to being recorded separately and summed by a virtual instrument (scenario II) we perform simulations of notes being played separately and simultaneously. We determine power spectra for select locations on the soundboard and investigate vibration patterns for both scenarios.

In Giordano's linear model of the soundboard, if two notes are applied simultaneously, the resultant displacements are identical to the sum of the displacements of the individual notes. Therefore, comparing the displacement amplitudes for the two scenarios yields no significant difference. However, the power spectra of the displacements, which are closely related to the sound intensities, are expected to be different for the two scenarios. The power spectrum of two notes simulated together is representative of simultaneously played notes on a piano. On the other hand, the sum of the power spectra of two notes simulated separately is representative of the output of pre-recorded piano tones in a virtual instrument.

In contrast to the linear soundboard model being considered so far, a non-linear model is expected to yield differences in the displacement amplitudes of the two scenarios. Chia [8] discusses non-linear models for vibrating plates of different symmetries and geometries. As a first step toward a non-linear soundboard model, we investigate the effect of one non-linear term on power spectra and displacement patterns.

Section 2 of this thesis introduces the hammer-and-string model and explains the numerical method for its simulation. Section 3 describes the linear model of the soundboard, the model for string-board interactions, and the finite difference method used in the simulations of the board. The non-linear extension of Giordano's model is discussed in section 3.4. In Section 4, we present and discuss our results. A summary and conclusions are presented in Section 5.

2 Hammer and String

2.1 Hammer and String Model

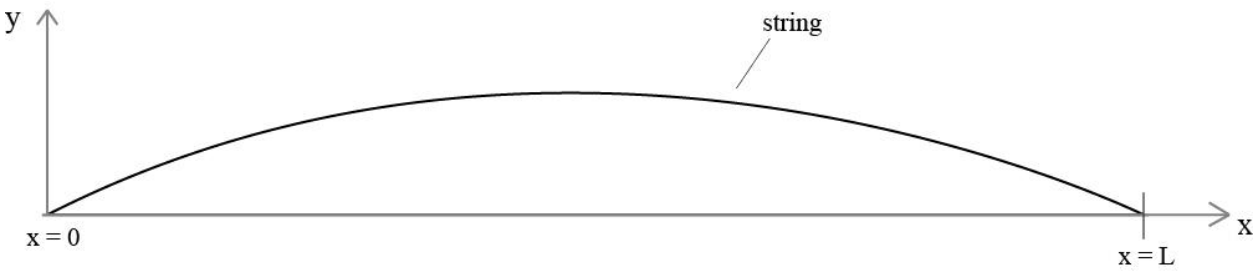

Figure 2: Illustration of the string model. The string (solid line) is fixed at $x = 0$ and $x = L$, and undergoes displacements in the y-direction.

Chaigne and Askenfelt [3] developed a physical model for a piano string struck by a hammer. This is the model we use to describe string vibrations and illustrate in Figure 2. The coordinate x runs parallel to the resting string while y is the string's displacement from the equilibrium position. The partial differential equation of motion for the string's displacement is

$$\frac{\partial y^2}{\partial t^2} = c^2 \frac{\partial^2 y}{\partial x^2} - \epsilon c^2 L^2 \frac{\partial^4 y}{\partial x^4} - 2b_1 \frac{\partial y}{\partial t} + 2b_3 \frac{\partial^3 y}{\partial t^3} + f(x.x_0, t), \tag{1}$$

Basic Wave Equation

Stiffness Term

Damping Terms

Applied Force Term

The left-hand side of the equation and the first term on the right make up the basic wave equation. Next is the fourth-order stiffness term, where ϵ is a string stiffness parameter, c is the transverse wave velocity, and L is the length of the string. After that, there are two damping

terms with constant damping coefficients b_1 and b_3. Lastly, there is the applied force term which is proportional to the hammer force. All terms beyond the basic wave equation are from Chaigne and Askenfelt [3]. The details of how the hammer force is applied to the string numerically is discussed in the Section 2.3, but the actual hammer force equation is

$$F_H(t) = K|\eta(t) - y(x_0, t)|^p \,, \tag{2}$$

where K is a coefficient of hammer stiffness, η is the hammer displacement, x_0 is the position where the hammer strikes the string, and $y(x_0, t)$ is the string displacement at x_0. The exponent, p, describes the non-linear hammer stiffness. It is due to the compression of the hammer's felt, which has memory of its compressed state [3]. Values for K and p are presented in Table 3.

2.2 String Boundary Conditions

The string is clamped at each end ($x = 0$ and $x = L$) so that the displacements are zero,

$$y(0, t) = y(L, t) = 0 \,. \tag{3}$$

The curvature of the strings at each end also vanishes to describe flat hinge points,

$$\frac{\partial^2 y}{\partial x^2}(0, t) = \frac{\partial^2 y}{\partial x^2}(L, t) = 0 \,. \tag{4}$$

2.3 Hammer and String Numerical Method

To create our numerical model for the string, a finite difference method is employed with discrete steps in time and space. The displacement at position x and time t is written as

$$y(i, n) \equiv y(x = i\Delta x, t = n\Delta t), \tag{5}$$

where i is the spatial counter and n is the time counter. The spatial step size follows from the number of string segments, $\Delta x = \frac{L}{n_x}$, where $n_x = 100$. The time step Δt is expressed as an inverse frequency, $\Delta t = 1/f_e$, where we use $f_e = 44000$ Hz for the note B2 and 12 x f_e for the note A5. To distinguish the time step in the string simulation from that in the soundboard simulation we add a subscript, Δt_{string}.

As described in reference [3], the PDE in equation (1) is solved by calculating the displacements at the next time steps from the displacements at the previous time steps. Except for points near the boundaries, the displacement of the i^{th} string segment at time step n+1 is calculated from

$$\begin{aligned} y(i,n+1) &= a_1 y(i,n) \\ &+ a_2 y(i,n-1) \\ &+ a_3[y(i+1,n) + y(i-1,n)] \\ &+ a_4[y(i+2,n) + y(i-2,n)] \\ &+ a_5[y(i+1,n-1) + y(i-1,n-1) + y(i,n-2)] \\ &+ \frac{[\Delta t^2 N F_H(n) g(i,i_0)]}{M_s}. \end{aligned} \tag{6}$$

The coefficients are defined as follows

$$a_1 = \left[2 - 2r^2 + \frac{b_3}{\Delta t} - 6\epsilon N^2 r^2\right]/D\ , \tag{7}$$

$$a_2 = \left[-1 + b_1 \Delta t + \frac{2b_3}{\Delta t}\right]/D, \tag{8}$$

$$a_3 = [r^2(1 + 4\epsilon N^2)]/D, \tag{9}$$

$$a_4 = \left[\frac{b_3}{\Delta t} - \epsilon N^2 r^2\right]/D, \tag{10}$$

$$a_5 = \frac{\left[-\frac{b_3}{\Delta t}\right]}{D}, \tag{11}$$

where N is the number of string segments and D is given by

$$D = 1 + b_1 \Delta t + \frac{2b_3}{\Delta t}\ . \tag{12}$$

The parameter r,

$$r = \frac{c\Delta t}{\Delta x}, \tag{13}$$

depends on the transverse wave velocity

$$c = \sqrt{\frac{T_s}{\mu}}. \tag{14}$$

ϵ is a numerical string stiffness parameter which was found by

$$\epsilon = \kappa^2 \left(\frac{E_S S}{T_s L^2}\right) \ , \tag{15}$$

where κ is the radius of gyration of the string, which is estimated as being half the string radius, and E_S is the Young's modulus of the string. *S* is the cross-sectional, circular area of the string, and *L* is the length of the string. The string length and diameter are in Table 1; elastic properties of the string are included in Table 3. Lastly, T_s is the string's tension which would be tuned on a real piano. For an ideal string, T_s can be calculated by equating the wave velocity in equation (14) with

$$c = \lambda f_1 \ . \tag{16}$$

Solving for T_s yields

$$T_s = \mu(\lambda f_1)^2 = \mu(2Lf_1)^2, \tag{17}$$

where λ, the wavelength of the fundamental is twice the string length, *L*, μ is the string's linear density, and f_1 is the fundamental frequency of the note being played. For the more realistic string model of equation (1), the tension force may need to be adjusted by a scaling factor to get the correct fundamental frequency.

The last term in equation (6) is the applied force,

$$\frac{[\Delta t^2 N F_H(n) g(i, i_0)]}{M_s}, \tag{18}$$

where M_s is the mass of the string and $g(i, i_0)$ is a spatial window, centered at $x_0 = i_0 \Delta x$ which distributes the force across the width of a hammer. The spatial window is defined as

$$g(i, i_0) = \frac{(x(i) - x_0 - w_H)(x(i) - x_0 + w_H)}{w_H^2}, \tag{19}$$

where w_H is the half-width of the hammer, half of the widest part of the hammer's felt head, as illustrated in Figure 3. Values for the felt width vary by note and are taken from Howard Piano Industries [9] and presented in Table 2.

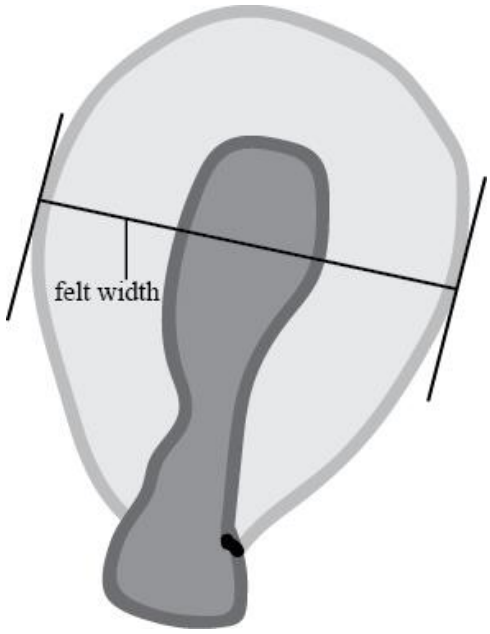

Figure 3: A sketch of a piano hammer head in side view. The dark area is the wooden portion and the light area around it is the felt. The measurement is taken from the widest part of the felt as indicated.

The discretized hammer force $F_H(n)$ is calculated from equation (2) for times between t = 0 and the contact time τ_0.

$$F_H(n + 1) = K|\eta(n) - y(i_0, n)|^p. \tag{20}$$

where $y(i_0, n)$ is the position of the string under the hammer and $\eta(n)$ is the position of the hammer at the previous time step, respectively. In first approximation, the velocity of the hammer is assumed to be constant during the contact time. Values for the contact time and initial velocity of the hammer are included in Table 3.

Lastly, the boundary conditions are handled by creating hinge ponts at each end of the string. To this end, one string segment is added to both ends of the string and the following boundary conditions are imposed

$$y(2,t) = y(nx-1,t) = 0 \tag{21}$$

$$y(1,t) = -y(3,t), \tag{22}$$

$$y(nx-2,t) = -y(nx,t), \tag{23}$$

which leaves $y(2,t)$ and $y(nx-1,t)$ equal to zero with no curvature, making up the physical ends of the string.

Note name	x_b/L Point at which the string meets the bridge as a ratio	f_1 Fundamental frequency	L Length of string [m]	l Position where hammer strikes string [m]	*aa* Ratio *L/l*	T_s String tension [N]	M_s Mass of string [kg]	D Diameter of the string [m]
A0		27.5	1.2392	0.1502	0.12	1350	0.360112	0.0015
A#2		116.5	0.8312	0.0992	0.12	625	0.013881	0.00095
B2	0.89	123.5	1.031	0.123	0.12	793	0.012578	0.000975
C3		130.8	1.0074	0.1201	0.12	747	0.01088	0.000975
C#3		138.6	0.9853	0.1174	0.12	773	0.010247	0.00095
D3		146.8	0.9641	0.1148	0.12	626	0.00752	0.00125
A4		440	0.3993	0.047	0.12	687	0.002236	0.00095
A5	0.71	880	0.2083	0.0219	0.11	672	0.001042	0.0009

Table 1: Piano string parameters. In our simulations, we use values for the fundamental frequency, f_1, the length L, the ratio *aa,* the mass of the string M_s, and the diameter of the string D from Stulov [10]. The positions, x_b, where the strings for B2 and A5 cross the bridge were measured by myself. Scale factors used to tune the tension in the string simulations. The scale factors for B2 and A5 are 0.94 an 0.86, respectively.

hammer felt widths	Note range on piano	Low end [inches]	High end [inches]	Low end [m]	High end [m]
	Low bass	1.25	1.3125	0.03175	0.033338
	High bass	1.1875	1.25	0.030163	0.03175
	Low tenor	1.09375	1.1875	0.027781	0.030163
	Mid tenor	1.03125	1.1875	0.026194	0.030163
	High tenor	0.96875	1.03125	0.024606	0.026194
	Low treble	0.84375	0.9375	0.021431	0.023813
	Mid treble	0.6875	0.8125	0.017463	0.020638
	High treble	0.5	0.6875	0.0127	0.017463

Table 2: The hammer felt widths from Howard [9] given in ranges for each section of notes on a piano. B2 would be high bass and A5 would be low/mid treble. The measurements are in both inches and meters.

$\boldsymbol{b_1}$ Damping constant	$\boldsymbol{b_3}$ Damping constant	$\boldsymbol{\tau_0}$ Hammer contact time [s]	$\boldsymbol{E_s}$ Young's modulus of string [N/m^2]	$\boldsymbol{p}$ Non-linear hammer stiffness component	**K** Hammer stiffness coefficient	$\boldsymbol{v_{H0}}$ Initial hammer velocity [m/s]
0.5	$6.25\text{x}10^{-9}$	0.00103	$2\text{x}10^{11}$	2.5	$4.5\text{x}10^{9}$	4.0

Table 3: Hammer and string parameters that are the same for all notes. Except for the hammer velocity, all values are from from Chaigne and Askenfelt [2, 3].

3 Soundboard

3.1 Soundboard Model

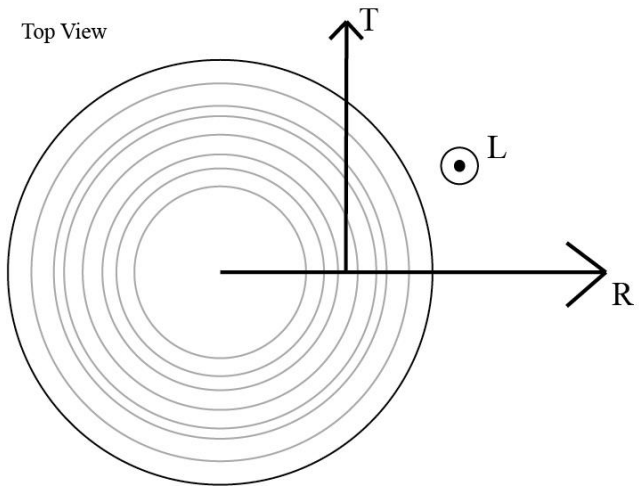

Figure 4: The coordinate system used in Bucur [3] when describing the elastic constants of wood. The sketch is of a tree stump seen from the top with the rings being represented by the lighter circles inside. The coordinates are relative to the wood grain.

Wood is a complicated material, partially because of its anisotropy. Bucur [11] describes how the elastic constants (Young's modulus, shear modulus, and Poisson's ratio) depend on the direction relative to the grain. If you picture a tree stump from above with its rings (Figure 4), there are three coordinates: *T* is the component which is tangential to the rings, *L* is parallel to the grain and moving upward (out of the page), and *R* is perpendicular to the grain, moving radially outward.

Things become simpler for the soundboard, however. The wood used is quarter sawn so that the tangential variation can be ignored and the only relevant directions for the elastic properties are *L* and *R*. In the geometry of our soundboard, shown in Figure 1, the grain (*L*) direction is parallel to the *x*-axis and the radial direction is parallel to the *y*-axis.

The soundboard itself is modeled as a square board of uniform thickness and mass density with the anisotropic elastic constants shown in Table 4. The bridge and ribs are represented as thin strips of increased thickness and with modified elastic constants; values for these parameters are in Table 6.

The equation of motion for the perpendicular displacement of the soundboard is given by the fourth-order PDE from Giordano [4, 5]

$$\rho_b h_b \frac{\partial^2 z}{\partial t^2} = -\beta' \frac{\partial z}{\partial t} - D_x \frac{\partial^4 z}{\partial x^4} - \left(D_x \nu_y + D_y \nu_x + 4D_{xy}\right) \frac{\partial^4 z}{\partial x^2 \partial y^2} - D_y \frac{\partial^4 z}{\partial y^4} + F_s(x_b, y_b), \tag{24}$$

where ρ_b is the density of the wood, $h_b$is the board thickness, β' is a decay coefficient, and ν_y, ν_x are Poisson's ratios. F_s represents the force of the string, which touches the bridge at position x_b, y_b.

The elastic properties of the material enter through the rigidity factors $D_x, D_y,$ and D_{xy}

$$D_x = \frac{h_b^3 E_x}{12\left(1 - \nu_x \nu_y\right)}, \tag{25}$$

$$D_y = \frac{h_b^3 E_y}{12\left(1 - \nu_x \nu_y\right)}, \tag{26}$$

$$D_{xy} = \frac{h_b^3 G_{xy}}{12}, \tag{27}$$

where E_x and E_y are Young's moduli in either direction and G_{xy} is the shear modulus. These values for the rigidity factor are used for all locations of the board that are not associated with the bridge or the ribs.

To put ribs into the system, we use a new thickness h_{rib} and a new Young's modulus E_{rib} for the direction parallel to the ribs. This yields different rigidity factors in the equation of motion at the location of the ribs, specifically,

$$D_{x,rib} = \frac{h_b^3 E_x}{12\left(1 - \nu_x \nu_y\right)}, \tag{28}$$

$$D_{y,rib} = \frac{(h_b + h_{rib})^3 E_{rib}}{12\left(1 - \nu_x \nu_y\right)}, \tag{29}$$

$$D_{xy,rib} = \frac{(h_b + h_{rib})^3 G_{xy}}{12} \ . \tag{30}$$

Notice that $D_{x,rib} = D_x$ because the ribs are so narrow that they do not affect the elastic properties in the perpendicular direction.

A similar method is applied to model the bridge, where the bridge height is added to the board height ($h_b + h_{bridge}$). Since the bridge is diagonal, the values of all three rigidity factors are modified to $D_{x,bridge}, D_{y,bridge,}$ and $D_{xy,bridge}$; values for the rib and bridge parameters are presented in Table 6.

3.2 Soundboard Boundary Conditions

The board is clamped at the edges such that

$$z(0, y, t) = z(x, 0, t) = z(L_b, y, t) = z(x, L_b, t) = 0, \tag{31}$$

where L_b is the side length of the board. Just like in the string model, the curvature is set to zero at the edges to create hinge points,

$$\frac{\partial^2 z}{\partial y^2}(0, y, t) = \frac{\partial^2 z}{\partial x^2}(x, 0, t) = \frac{\partial^2 z}{\partial y^2}(L_b, y, t) = \frac{\partial^2 z}{\partial x^2}(x, L_b, t) = 0. \tag{32}$$

3.3 Soundboard Numerical Method

Once again, we are using a finite difference method to solve the PDE. The primary source for this method is Giordano [4] and [7]. The displacement is perpendicular to the board and written as

$$z(i, j, n) \equiv z(x = i\Delta x, y = j\Delta y, t = n\Delta t), \tag{33}$$

where *i* and *j* are the spatial counters for *x* and *y*, and *n* is the time counter with the appropriate step sizes $\Delta x, \Delta y,$ and Δt. Values for Δx and Δy are included in Table 6, the size of the time step, $\Delta t = \Delta t_{board}$, is shown in Table 5. See also Figure 9, which contains an illustration of the soundboard as a grid.

The displacement at time step $n + 1$ is calculated from the displacements at earlier times and the applied force due to the strings, F_s

$$\begin{aligned} z(i,j,n+1) = {} & a_1 z(i,j,n) + a_2 z(i,j,n-1) \\ & + a_3[z(i+2,j,n) - 4z(i+1,j,n) + 6z(i,j,n) - 4z(i-1,j,n) \\ & + z(i-2,j,n)] \\ & + a_4[z(i,j+2,n) - 4z(i,j+1,n) + 6z(i,j,n) - 4z(i,j-1,n) \\ & + z(i,j-2,n)] \\ & + a_5[z(i+1,j+1,n) + z(i+1,j-1,n) + z(i-1,j+1,n) \\ & + z(i-1,j-1,n) - 2z(i+1,j,n) - 2z(i-1,j,n) - 2z(i,j+1,n) \\ & - 2z(i,j-1,n) + 4z(i,j,n)] \\ & + a_6 F_s(i,j,n) \quad . \end{aligned} \tag{34}$$

The coefficients are

$$a_1 = \frac{2}{1+\beta} \quad , \tag{35}$$

$$a_2 = \frac{-1+\beta}{1+\beta} \quad , \tag{36}$$

$$a_3 = -\frac{D_x(\Delta t)^2}{\rho_b h_b (\Delta x)^4} \quad , \tag{37}$$

$$a_4 = -\frac{D_y(\Delta t)^2}{\rho_b h_b (\Delta y)^4} \quad , \tag{38}$$

$$a_5 = -\frac{D_{xy}(\Delta t)^2}{\rho_b h_b (\Delta x)^2 (\Delta y)^2} \quad , \tag{39}$$

$$a_6 = \frac{(\Delta t)^2}{\rho_b h_b \Delta x \Delta y} \quad , \tag{40}$$

where β, the dissipation constant, is defined as

$$\beta = \frac{R\Delta t}{2\rho_b h_b} \quad , \tag{41}$$

with R being the dissipation scale factor, which was set to $R = 4000$. The rigidity factors in equations (37)– (39) are modified at the locations of the bridge and the ribs.

The force F_s on the board, at the bridge location, is described by the vertical component of the tension in the string,

$$F_s = T_{s,y} = T_s \sin\alpha \quad , \tag{42}$$

where the angle α is defined in Figure 5. Please note that Figure 5 uses the coordinates of the string defined in Figure 2. With the notation in Figure 5, $\sin\alpha$ is calculated from

$$\sin\alpha = \frac{\Delta y_{string}}{\sqrt{(\Delta x)^2 + \left(\Delta y_{string}\right)^2}}. \tag{43}$$

Δy_{string} changes with time since it depends on the string displacement, while Δx is constant. In practice, we perform a simulation of the string being played and store data of the string force as a function of time. These data are used in a separate simulation to create vibrations in the soundboard. Table 5 shows the sampling rate and values for the time steps in both simulations, which must be compatible.

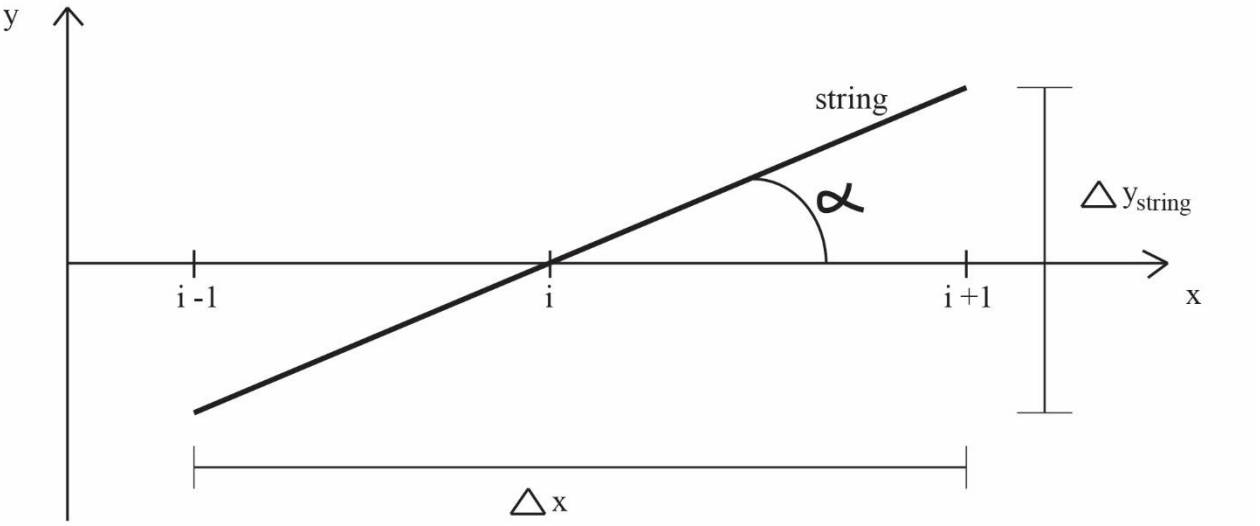

Figure 5: Illustration of the geometry used to calculate the string force F_s. For the string system, *y* is the string displacement and *x* runs parallel along the resting string. $x_b = i\Delta x$ is the location where the string touches the bridge. The angle α describes the angle between the moving string at x_b and the resting string.

Lastly, the boundary conditions on the board are implemented by setting

$$z(2, y, t) = z(\mathrm{x}, 2, t) = z(nx - 1, y, t) = z(\mathrm{x}, ny - 1, t) = 0\,, \tag{44}$$

and by creating flat hinge points at the edges:

$$z(1, y, t) = -z(3, y, t)\,, \tag{45}$$

$$z(x, 1, t) = -z(x, 3, t)\,, \tag{46}$$

$$z(nx - 2, y, t) = -z(nx, y, t)\,, \tag{47}$$

$$z(x, ny - 2, t) = -z(x, ny, t)\,. \tag{48}$$

Material of board	$\boldsymbol{\rho_b}$ Density [$\mathrm{kg/m^3}$]	$\boldsymbol{E_x}$ Young's modulus for *x*-direction [$10^8\mathrm{N/m^2}$]	$\boldsymbol{E_y}$ Young's modulus for *y*-direction [$10^8\mathrm{N/m^2}$]	$\boldsymbol{G_{xy}}$ Shear modulus [$10^8\mathrm{N/m^2}$]	$\boldsymbol{\nu_x}$ Poisson's ratio for *x*-direction	$\boldsymbol{\nu_y}$ Poisson's ratio for *y*-direction
Spruce	440	6.9	159	7.5	0.028	0.44

Table 4: Elastic parameters for the soundboard model used in this work. The values are from table 4.1 in Bucur [11] and represent spruce, which seems to be the most common type of wood for a soundboard.

	$\boldsymbol{f_e}$ Sampling rate [Hz]	String program step-size scale factor	$\boldsymbol{\Delta t_{string}}$ String program step-size [s]	Soundboard program step-size scale factor	$\boldsymbol{\Delta t_{board}}$ Soundboard program step-size [s]
B2	44000	1	1/44000	40	1/1760000
A5	44000	12	1/528000	40	1/1760000

Table 5: Sampling rate of the string force and time step values in the string and soundboard simulations. The sampling rate f_e sets the time scale for all simulations. To calculate time steps for the string and the soundboard simulations that are compatible with each other, integer scale factors are employed.

L_b side length of the soundboard [m]	h_b Soundboard thickness [m]	h_{rib} Rib thickness [m]	h_{bridge} Bridge thickness [m]	E_{rib} Modified Young's Modulus for ribs	E_{bridge} Modified Young's Modulus for bridge	$\Delta x = \Delta y$ Spatial step-size [m]
1	0.01	0.01	0.033	1.5 x E_y	1.0 x E_y	0.01

Table 6: Size and elastic parameters for the soundboard, ribs and the bridge. These parameters are from Giordano [4, 5] aside from the bridge height, which I measured myself.

3.4 Soundboard Non-linearity

Chia [8] discusses a non-linear model for an orthotropic plate, such as the soundboard model in this work. The nonlinear model involves lateral as well as perpendicular displacements and leads to a set of coupled PDEs.

As a first step toward a non-linear model for the soundboard, we neglect lateral displacements and identified the largest non-linear term in the PDE for the perpendicular displacement. This term is shown in equation (49) and is added to the right-hand-side of the soundboard PDE in equation (24).

$$+\frac{h_b}{1-\nu_x\nu_y}\left[\frac{1}{2}\left(\frac{\partial z}{\partial y}\right)^2\left(\nu_x E_y\frac{\partial^2 z}{\partial x^2}+E_y\frac{\partial^2 z}{\partial y^2}\right)\right] \tag{49}$$

To implement this non-linearity numerically, it is split into two terms, one for each of the second-order derivatives. Now, to be added to the right-hand-side of equation (34) are the new terms

$$+a_7\left[\big(z(i,j+1,n)-z(i,j-1,n)\big)^2*\big(z(i+1,j,n)-2z(i,j,n)+z(i-1,j,n)\big)\right] \tag{50}$$
$$+a_8\left[\big(z(i,j+1,n)-z(i,j-1,n)\big)^2*\big(z(i,j-1,n)-2z(i,j,n)+z(i,j-1,n)\big)\right] \quad ,$$

with the new coefficients

$$a_7=\frac{(\Delta t)^2}{(\Delta x)^4}\,\frac{h_b}{1-\nu_x\nu_y}\frac{1}{16}\,\nu_x\,E_y \quad , \tag{51}$$

and

$$a_8 = \frac{(\Delta t)^2}{(\Delta x)^4} \frac{h_b}{1 - \nu_x \nu_y} \frac{1}{16} E_y \quad . \tag{52}$$

As before, elastic parameters for ribs and bridge are substituted at the proper locations.

4 Results & Discussion

In this section we present results of our work. The first step is the simulation of the piano strings that are played. From the vibrations of the string at the bridge location, the force of the string on the bridge is calculated and stored to be used as the input for the soundboard simulations.

4.1 Results from the String Model

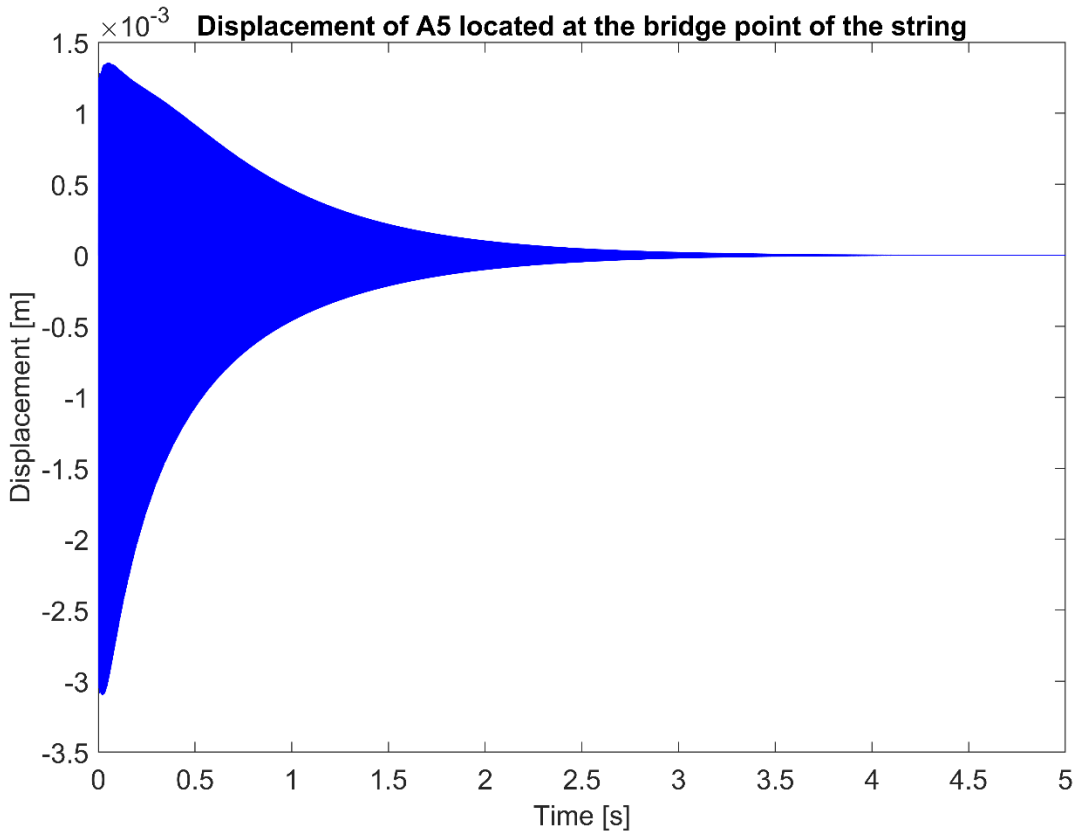

Figure 6: Displacement versus time for the note A5 being played on the string model. The graph shows the displacement at the point on the string at which it would be resting on the bridge.

In Figure 6 we present simulation results for the displacement of the A5 string at the bridge location as a function of time. The hammer is in contact with the string between time t = 0 and $t = \tau_0 = 0.00103$ s. The graph shows the long time behavior of decaying vibrations. Figure 7 shows a close-up of Figure 6, illustrating the nearly sinusoidal motion at intermediate times.

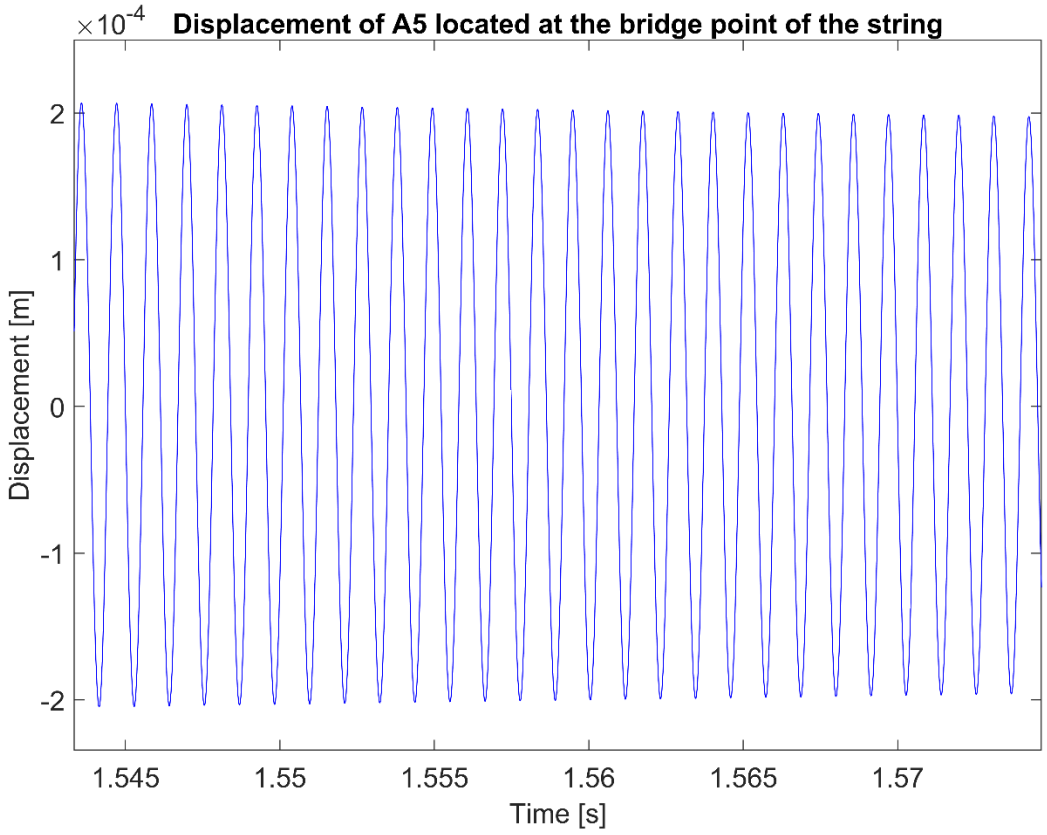

Figure 7: A close-up of Figure 6.

In Figure 8, we present simulation results for the B2 string. Compared to the A5 string, the vibrations for B2 show less damping and a higher amplitude for the same hammer velocity.

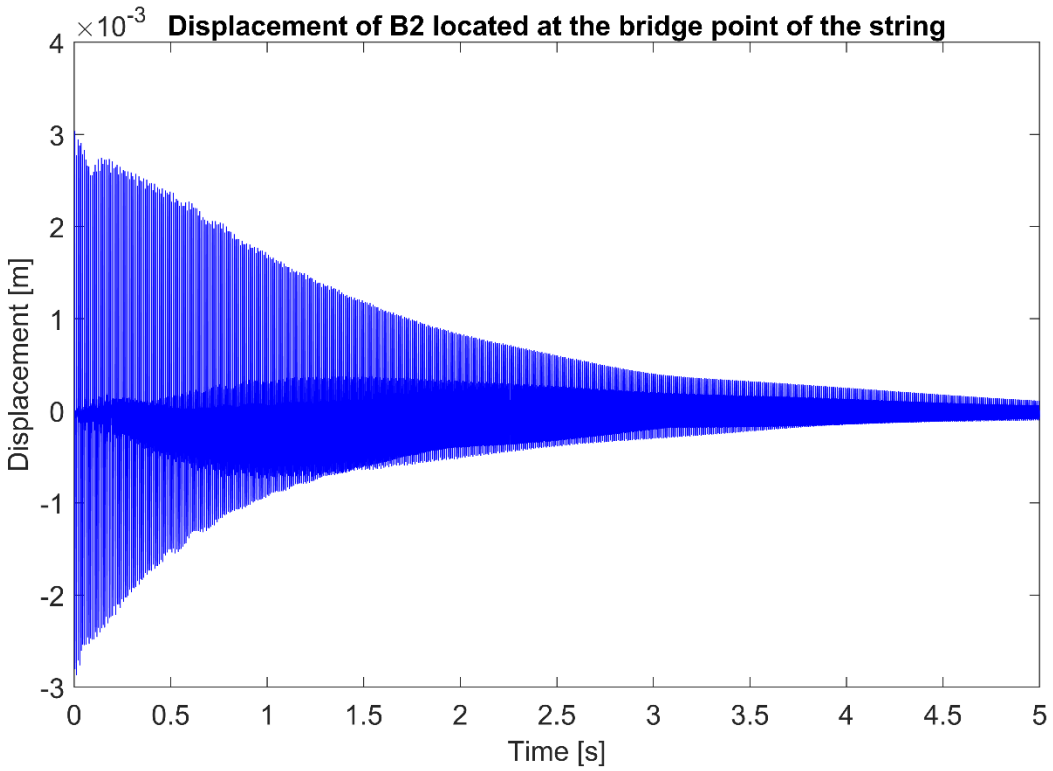

Figure 8: Displacement versus time for the note B2 being played on the string model. The graph shows the displacement at the point on the string at which it would be resting on the bridge.

4.2 Linear Soundboard - Locational Dependence

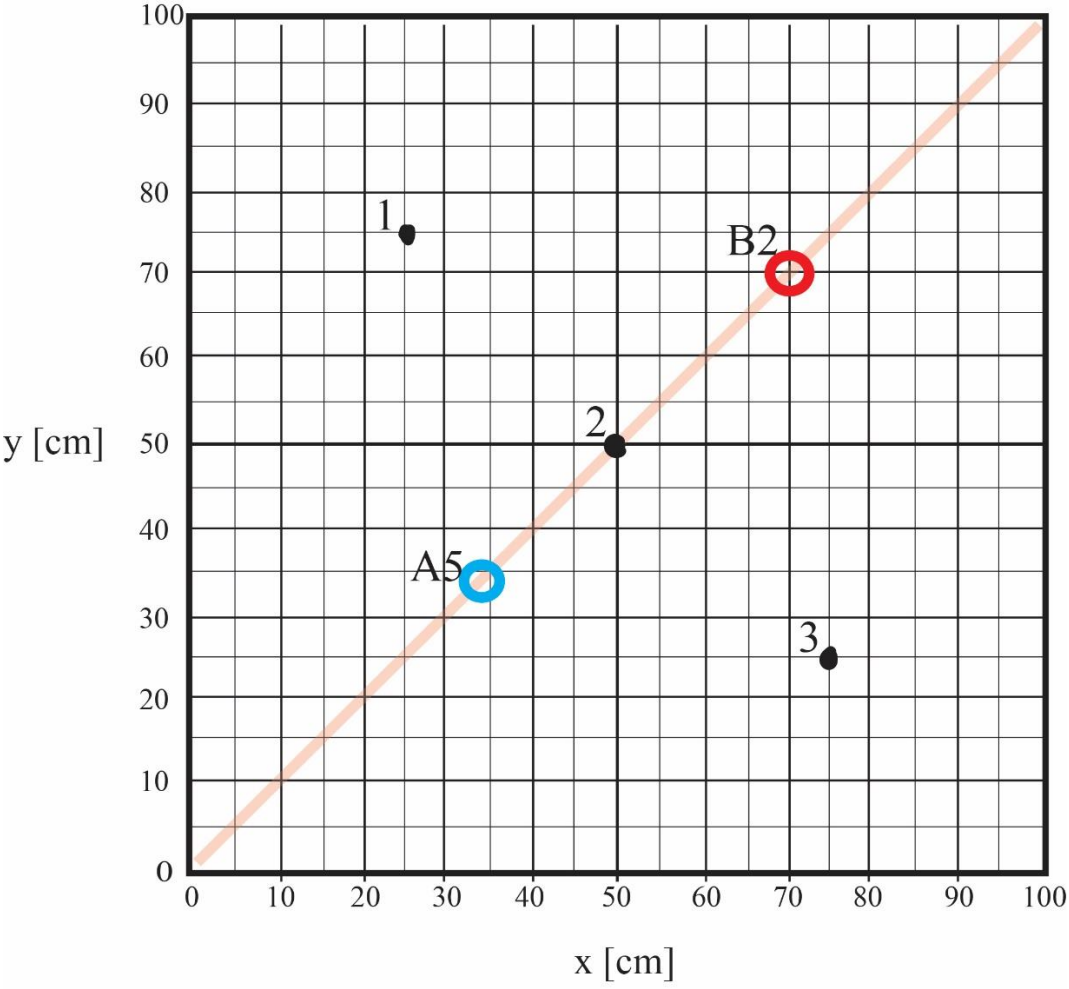

Figure 9: A coordinate grid of the soundboard, which contains 100 x 100 points. The *y* axis is on the side, where the piano keys would be located. The bridge is drawn in with a faint, thick line along the diagonal, $y = x$. The rings located at (34, 34) and (70, 70) mark the positions where strings B2 and A5 touch the bridge; these are the locations of the applied string force for the notes. The points indicate the locations at which we sample the board's displacement for analysis. Location "1" has coordinates (25, 75), "2" is at (50, 50) on the bridge, and location "3" is at (75, 25).

To start, we look at simulation results from each location (1, 2, and 3) when both notes (B2 and A5) are being played at the same time. This allows us to identify the location that will be used for further analysis. Figure 10, Figure 11, and Figure 12 show the board displacements at locations 1, 2, and 3, respectively.

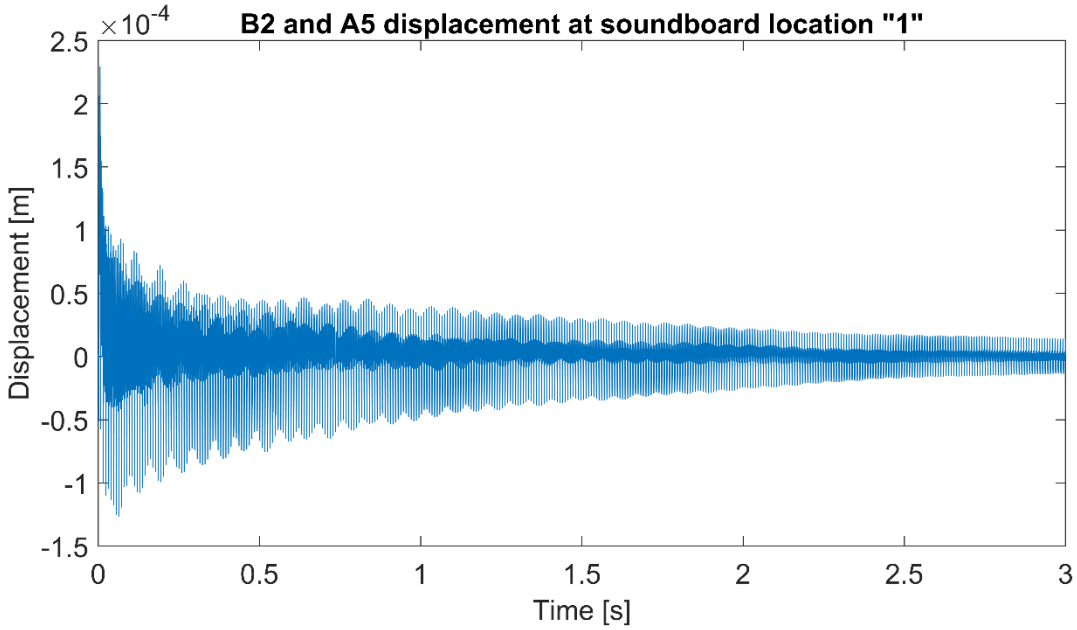

Figure 10: The displacement of the soundboard as a function of time at location 1 for both notes being played simultaneously. The denser area in the wave pattern is the signal of the note A5 which is of a higher frequency.

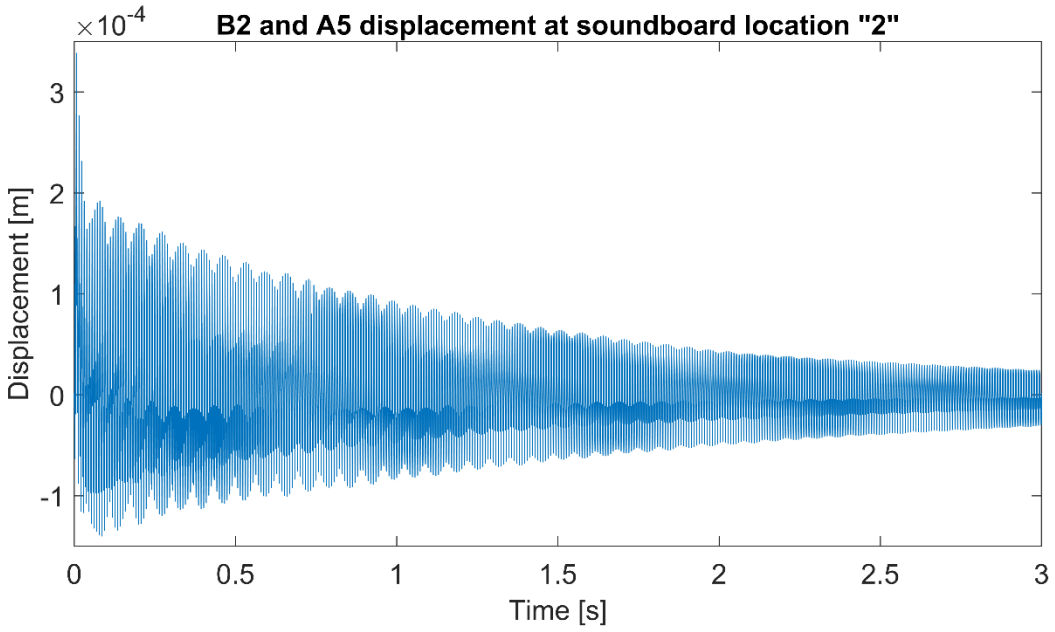

Figure 11: Soundboard displacement of both notes at location 2 which is on the bridge, in the center of the soundboard.

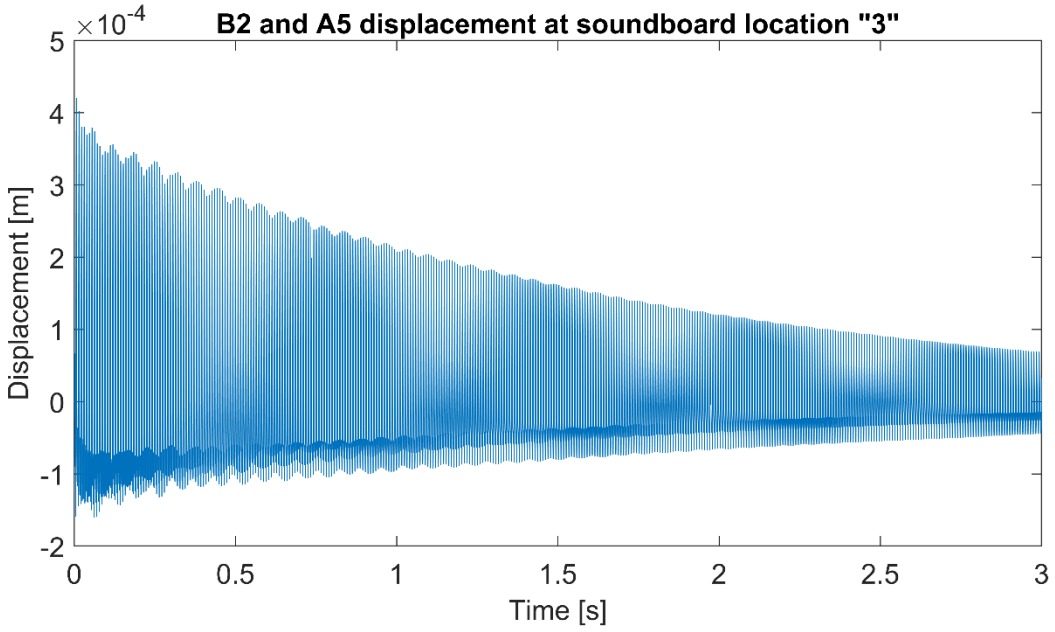

Figure 12: Soundboard displacement of both notes at location 3.

A comparison of Figure 10, Figure 11, and Figure 12 shows that the amplitudes are comparable for locations 2 and 3 and smaller at location 1. This is primarily due to a smaller signal from note B2 at location 1, as confirmed by evaluating power spectra at these locations (not shown).

Location 1 is the one at which we analyze the board displacement from now on since it has the best signal ratio between A5 and B2.

4.3 Linear Soundboard – Solo Note Analysis

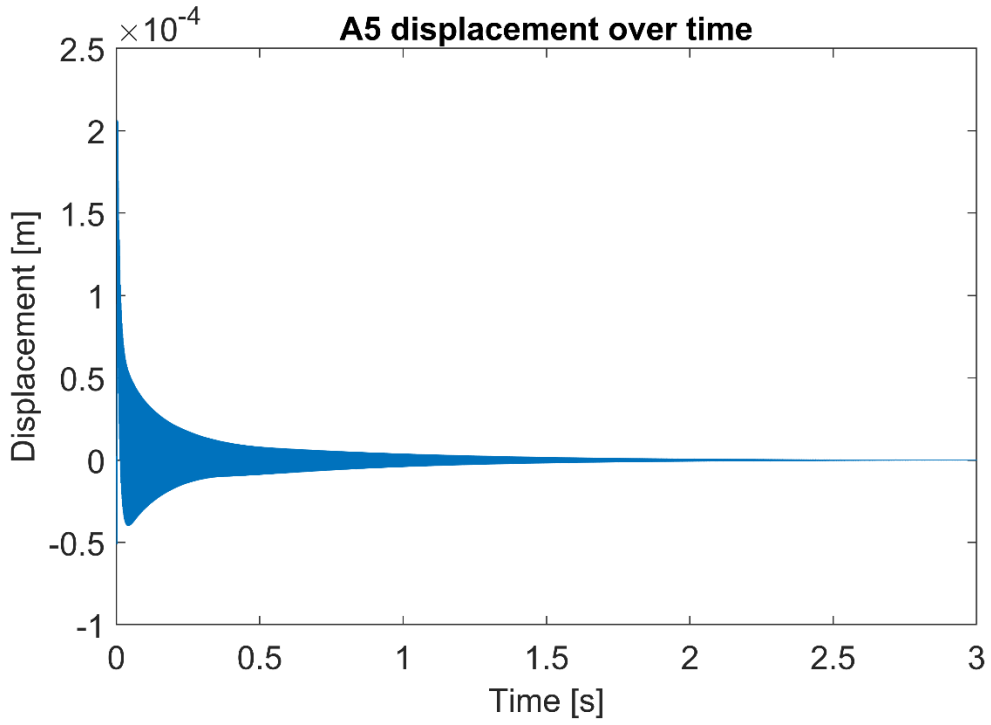

Figure 13: The soundboard displacement as a function of time while only the note A5 is being played. This data is collected from the standard soundboard location 1.

In this section, we compare the board displacements and power spectra at location 1 of Figure 9 for the notes A5 and B2 being played separately. Figure 13 and Figure 14 show the displacement as a function of time and the power spectrum for note A5, Figure 15 and Figure 16 show the corresponding results for B2.

To generate the power spectra, a fast Fourier transform (FFT) was applied to the displacement as a function of time and the amplitudes of the Fourier components were squared. The frequencies have discrete values f_n and the power amplitudes are called $G(f_n)$.

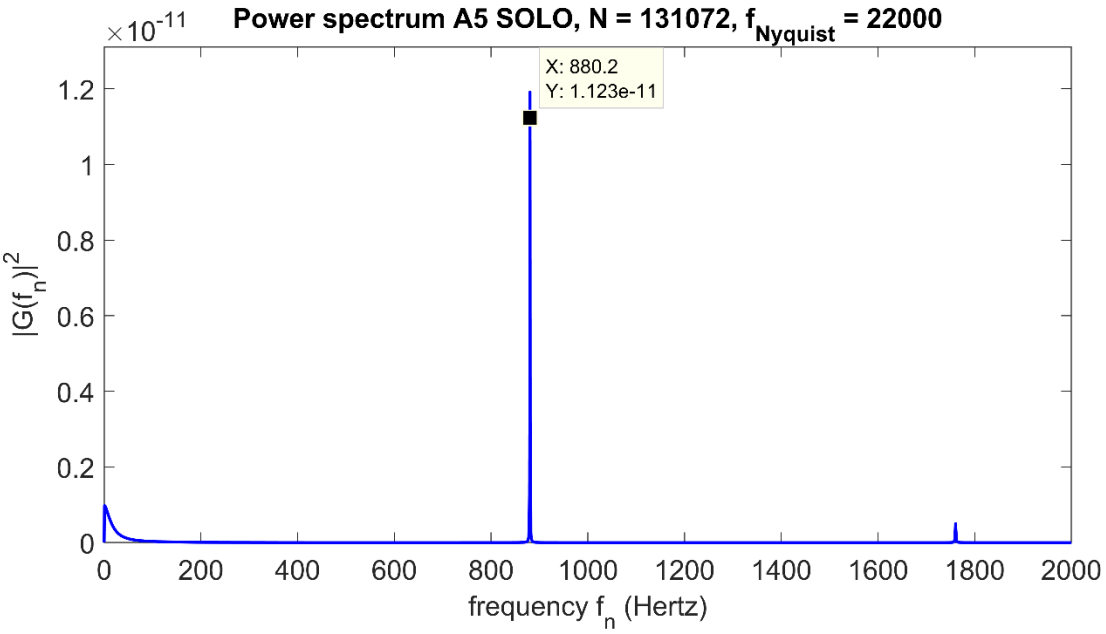

Figure 14: Power spectrum of the data from Figure 13, f_n and G are the discrete frequencies and Fourier components, respectively. The fundamental peak is located at approximately 880.2 Hz which is correct for A5. There is also a partial peak just under 1800 Hz which is to be expected since it is double the fundamental frequency.

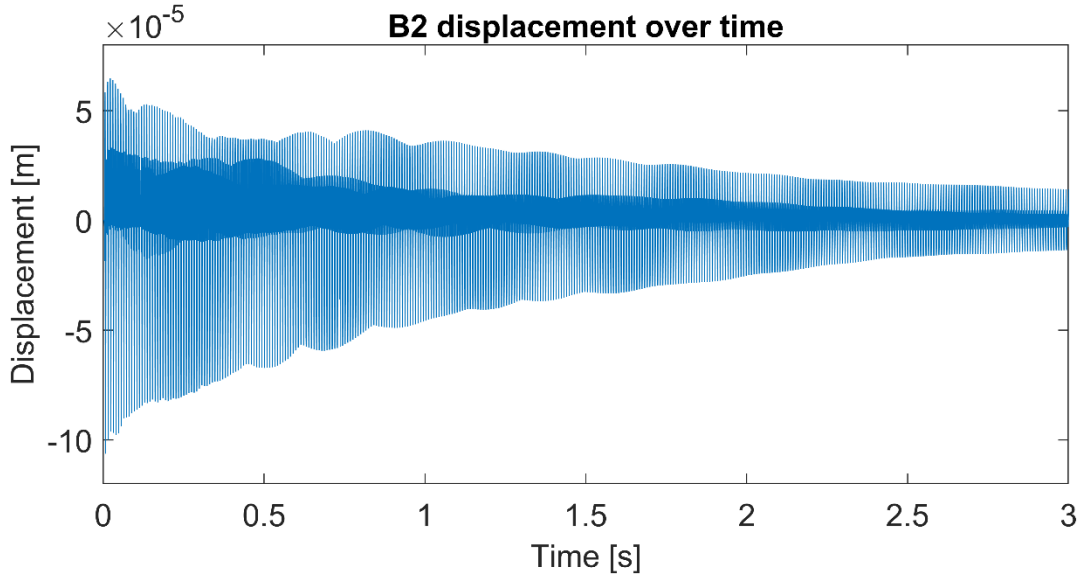

Figure 15: The soundboard displacement as a function of time while only the note B2 is being played.

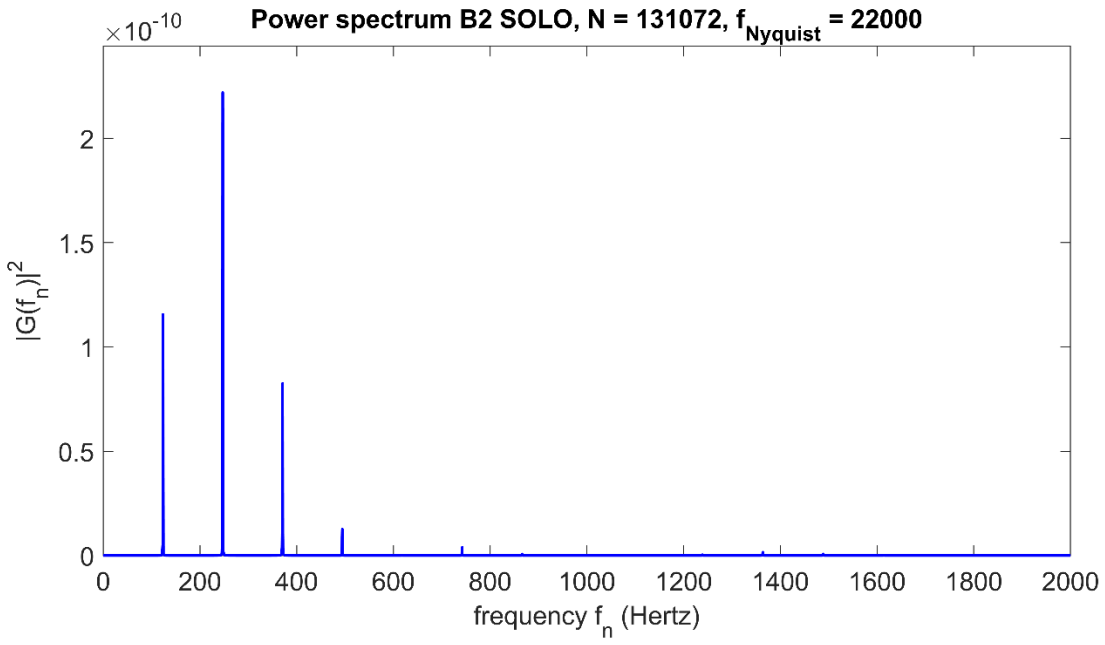

Figure 16: Power spectrum of the data from Figure 15, f_n and G are the discrete frequencies and Fourier components, respectively. The first peak at 123.5 Hz indicates the fundamental frequency, which is correct for B2. The other peaks are at multiples of the fundamental.

The power spectrum for B2 in Figure 16 shows a peak at the fundamental frequency and partials at multiples of the fundamental. Notice that the first partial has greater power than the fundamental. This is not unexpected: due to the physical size of the strings and the soundboard, it is common for bass notes to have less power in the fundamental than the first partial.

Figure 13 and Figure 15 show that the amplitude of note A5 is smaller, and the decay time shorter than for B2. The power spectrum of A5 in Figure 14 has a strong peak at the fundamental $f_{A5} = 880.2$ Hz and a smaller peak at a partial at twice the fundamental frequency. The contributions of the power spectrum at any low frequencies are due to the decaying envelope of the vibration.

4.4 Linear Soundboard – Comparing Pre-recorded Sounds

As explained in the Introduction, our goal is to create power spectra that are representative of a note's recorded audio signal. Adding the power spectra of the solo notes is a model for a virtual instrument combining pre-recorded samples for playback of a chord. I will refer to the added power spectra of the "pre-recorded" notes as played post-summed. The post-summed notes will be compared to the power spectrum of two notes that were played at the same time.

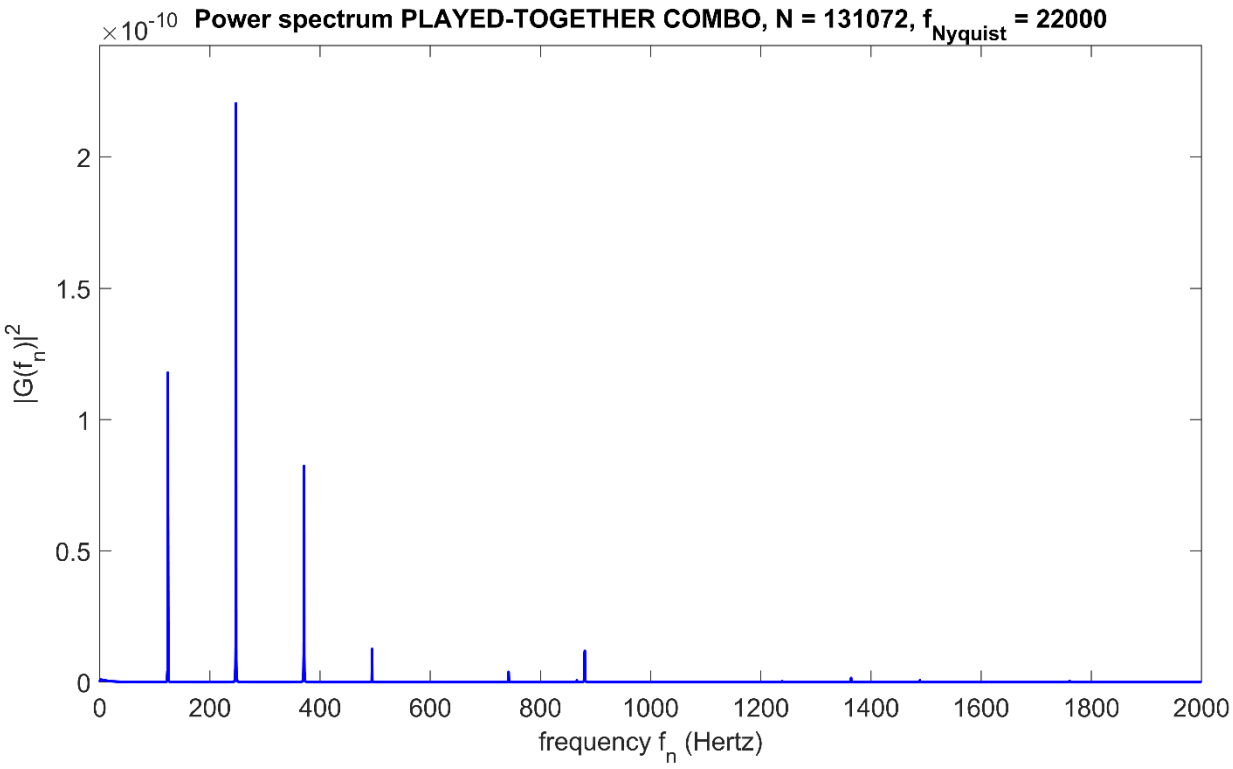

Figure 17: Power spectrum for the displacement function of the two notes B2 and A5 being played on the soundboard at the same time. Signatures of both notes are present, although A5's signal is much smaller.

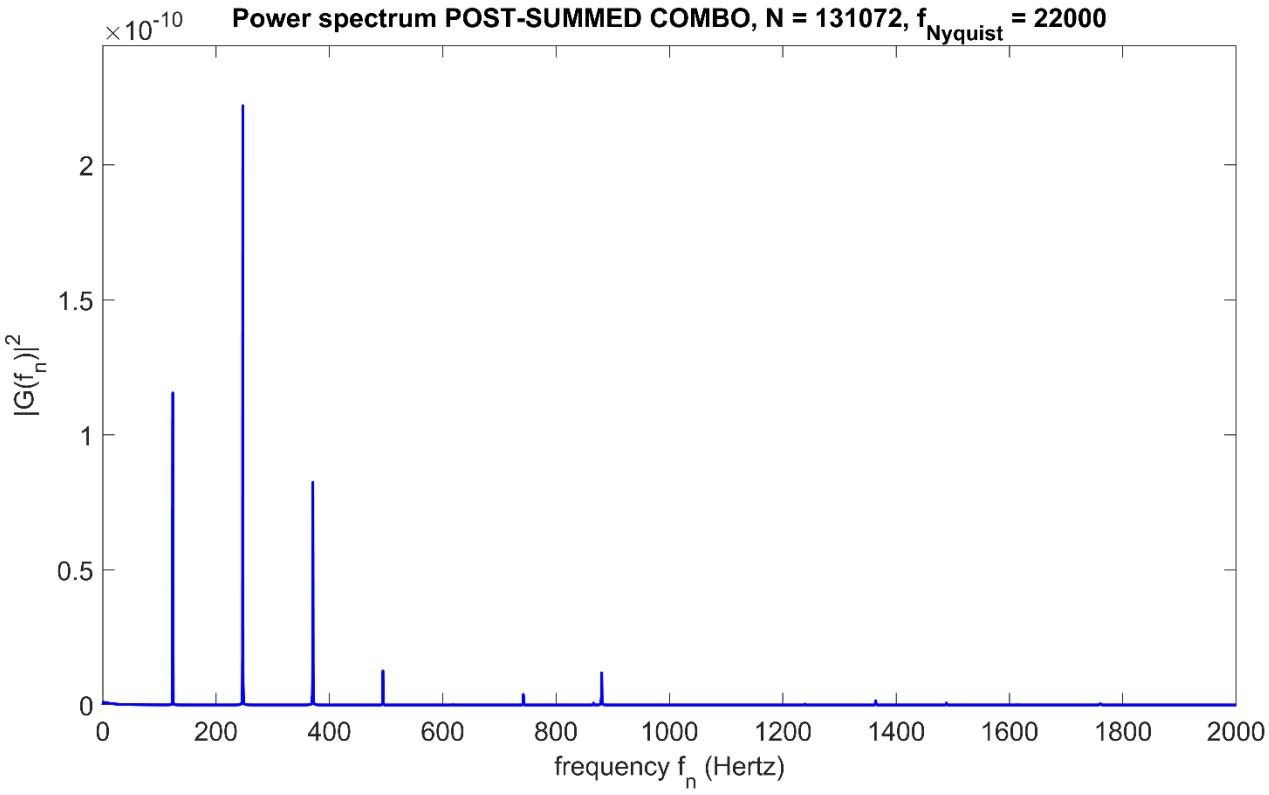

Figure 18: Power spectrum for the post-summed notes. The power spectrum looks very similar to that of the simultaneously played notes in Figure 17.

Figure 17 shows the power spectrum for two notes being played together. The spectrum is dominated by the signal from the bass note, B2, which is much stronger than that of the note A5. The power spectrum of the post-summed notes in Figure 18 looks very similar to the spectrum of the notes being played simultaneously. To investigate how they differ, we present in Figure 19 the absolute difference of the spectra in Figure 17 and Figure 18. While the differences are about a factor 100 smaller than the original spectra, they are significant. The peaks in Figure 19 occur at the correct frequencies and are too large to be numerical artifacts. Figure 19 shows that the differences between the scenarios are subtle but quantifiable.

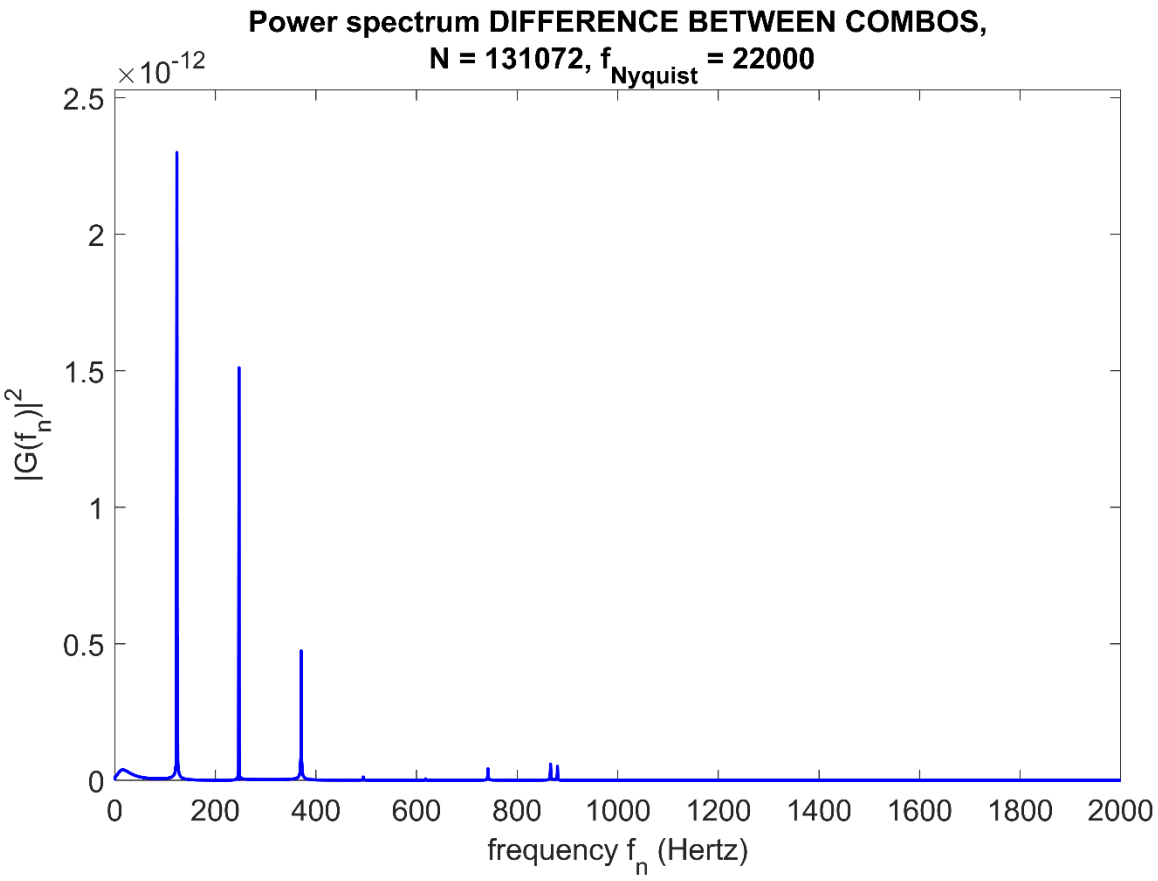

Figure 19: The absolute difference between the power spectra of Figure 18 and Figure 17.

4.5 Linear Soundboard – Vibration Patterns

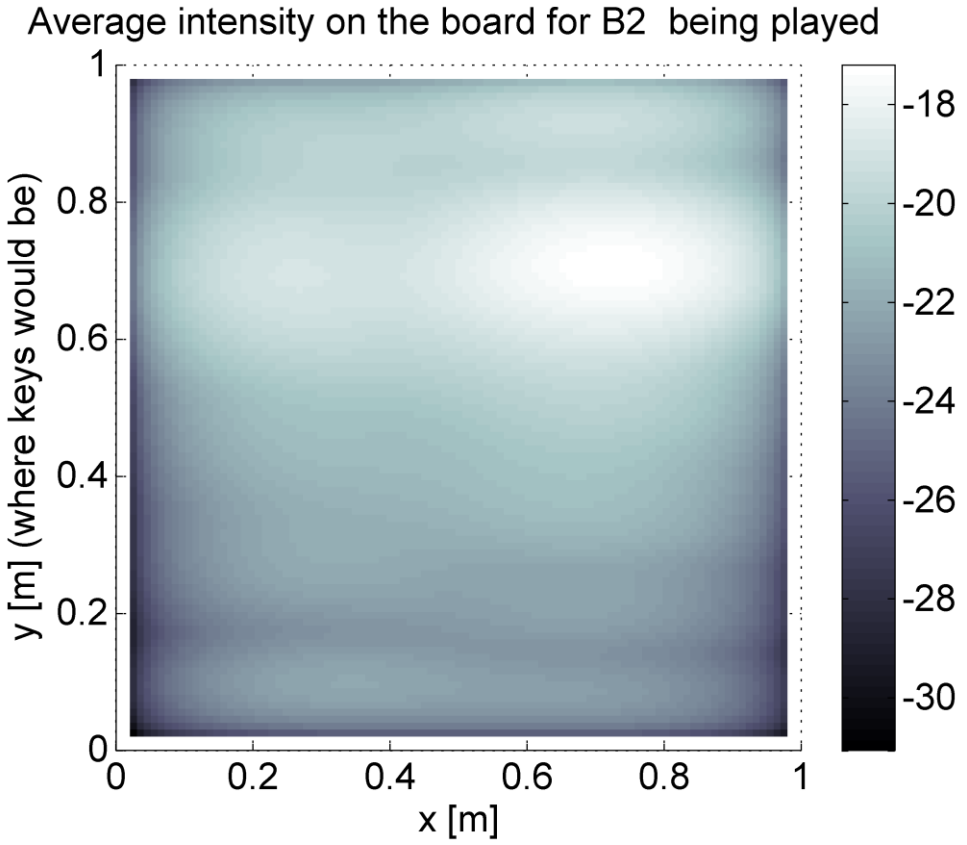

Figure 20: A map of the soundboard showing a vibration pattern that is proportional to the intensity [a.u] in log scale when only the note B2 is being played.

To investigate how the soundboard as a whole vibrates when notes A5 and B2 are played, we calculated time averaged values of the square displacements, which are proportional to the intensity, for all positions on the board.

Figure 20 shows the vibration pattern when the note B2 is played. The colors indicate, in log scale, the square displacements averaged over about 0.05 s starting at 0.05 s. This time window captures the signal after the interaction between hammer and string is over and before the signal decreases significantly due to damping. Figure 21 shows the vibration pattern for note A5.

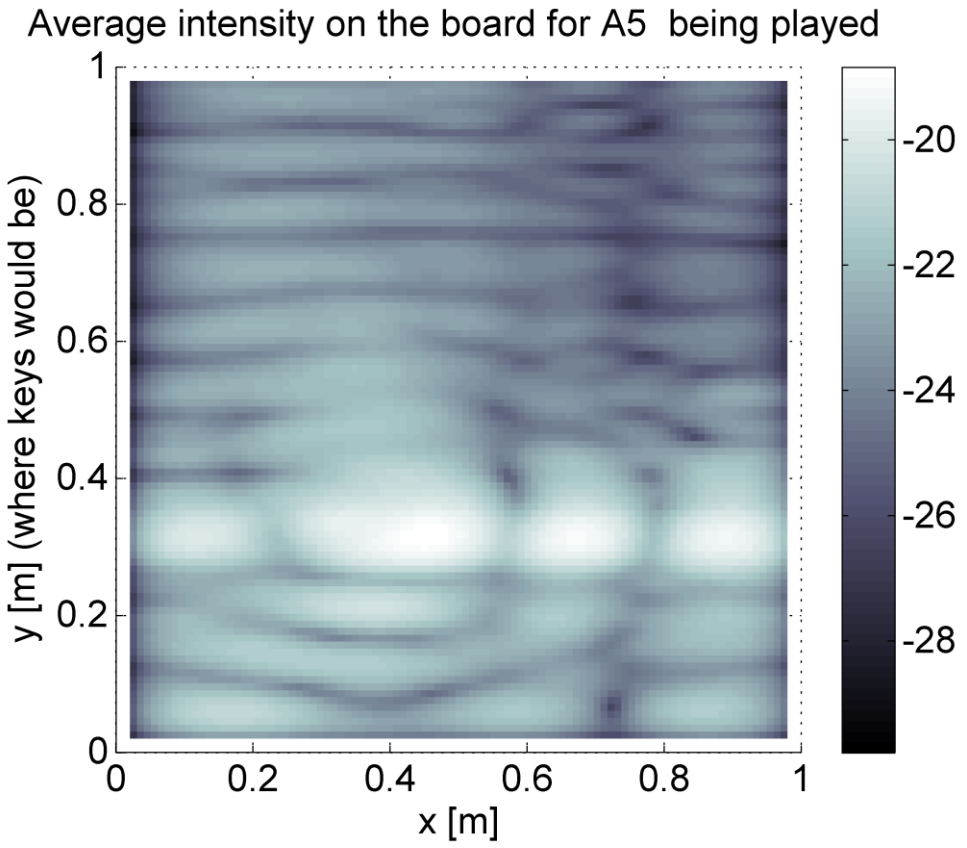

Figure 21: A map of the soundboard showing a vibration pattern that is proportional to the intensity [a.u] in log scale when only the note A5 is being played.

The brightest spots, corresponding to the highest intensities, in Figure 20 and Figure 21 are quite close to the locations where the string force for each note is applied.

The pattern for A5 shows a series of dark lines parallel to the x-axis. These lines represent nodal lines of the standing wave on the board. Except near y = 0.3, the pattern has little variation along the x – direction. The pattern for B2 shows vibration modes of lower order than that for A5. This is to be expected since B2 is a note of lower frequency and, thus, longer wavelength.

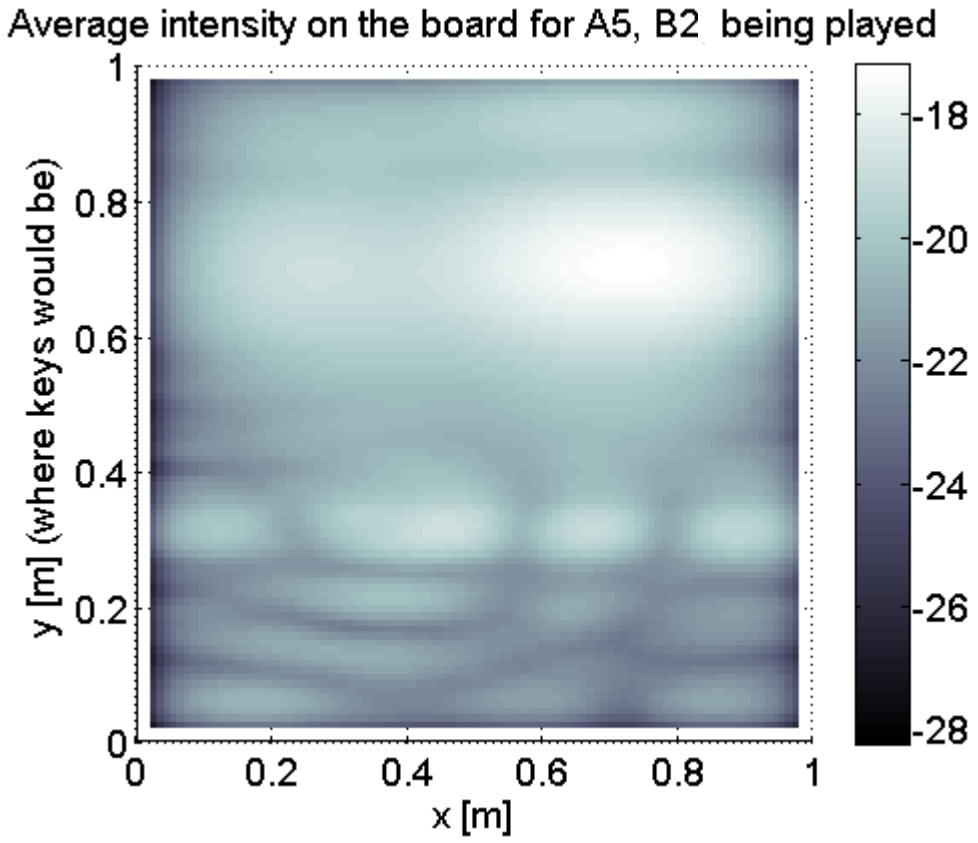

Figure 22: A map of the soundboard showing a vibration pattern that is proportional to the intensity [a.u] in log scale when both B2 and A5 are being played together.

Figure 22 shows the vibration pattern when notes A5 and B2 are played at the same time. The intensity distribution shows signatures from notes B2 and A5 in the upper and lower region of the board, respectively.

4.6 Non-linear Soundboard – Power Spectra

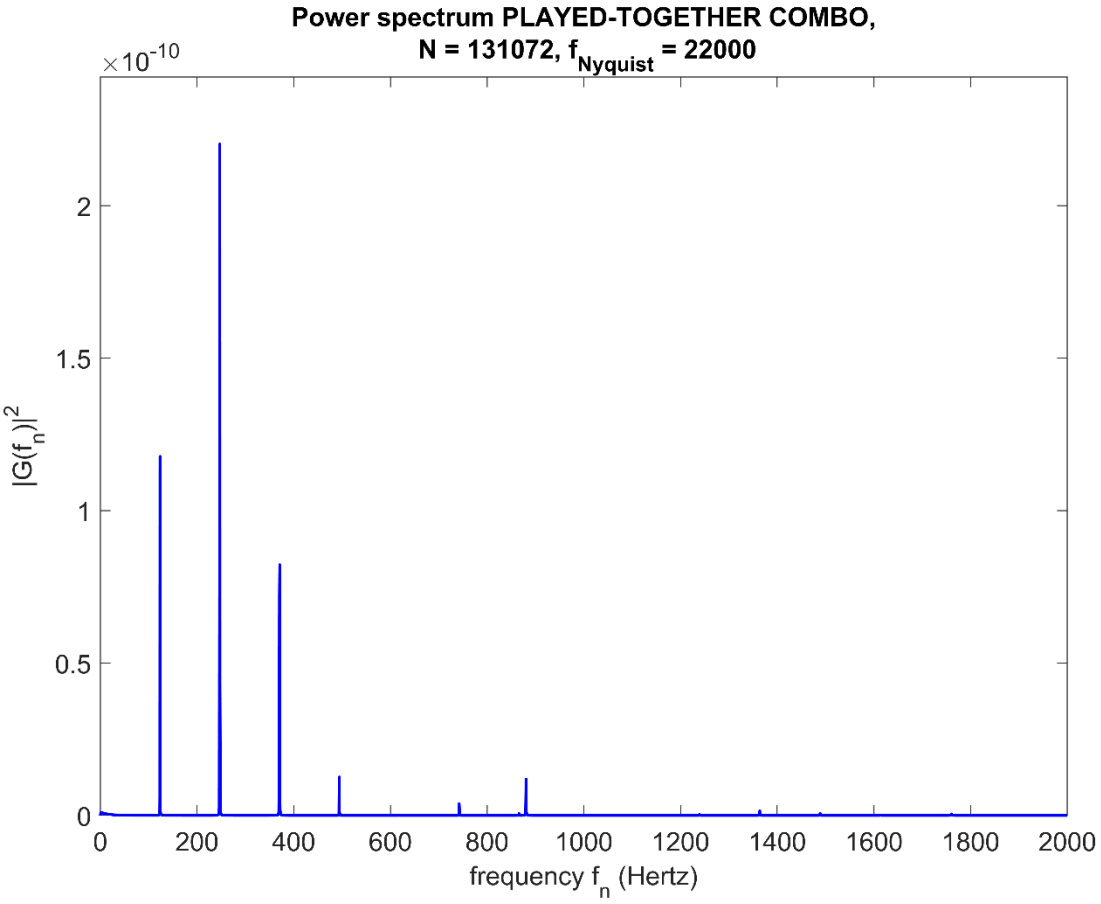

Figure 23: Power spectrum from the displacement of the two notes B2 and A5 being played on the non-linear soundboard at the same time.

In this section, we repeat the power spectra analysis for simulations with the non-linear soundboard model.

Figure 23 shows the power spectrum from simulations of the non-linear model when notes B2 and A5 are played together. Figure 24 shows the power spectrum for the post-summed B2, A5 combination, and Figure 25 shows the absolute difference between the power spectra in Figure 23 and Figure 24.

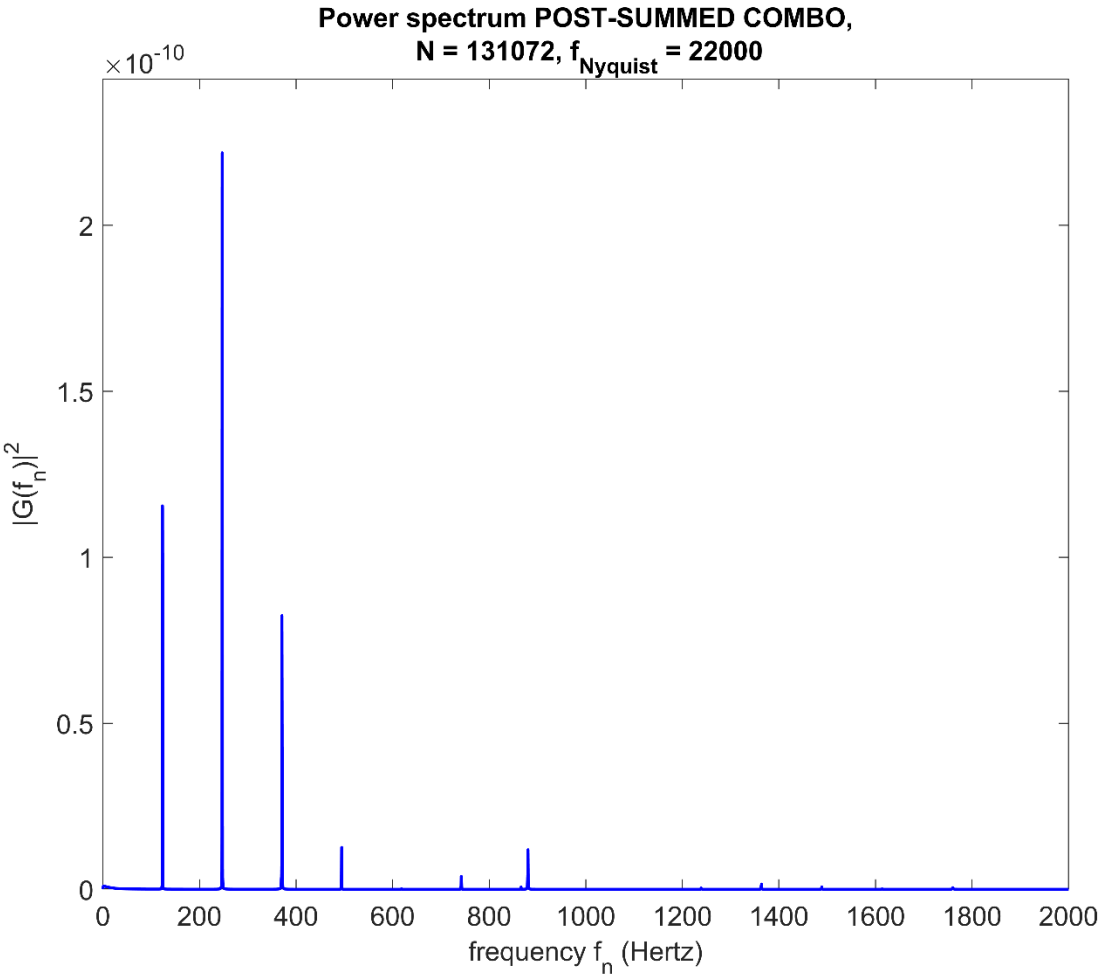

Figure 24: Power spectrum for the post-summed notes from simulations of the non-linear board model.

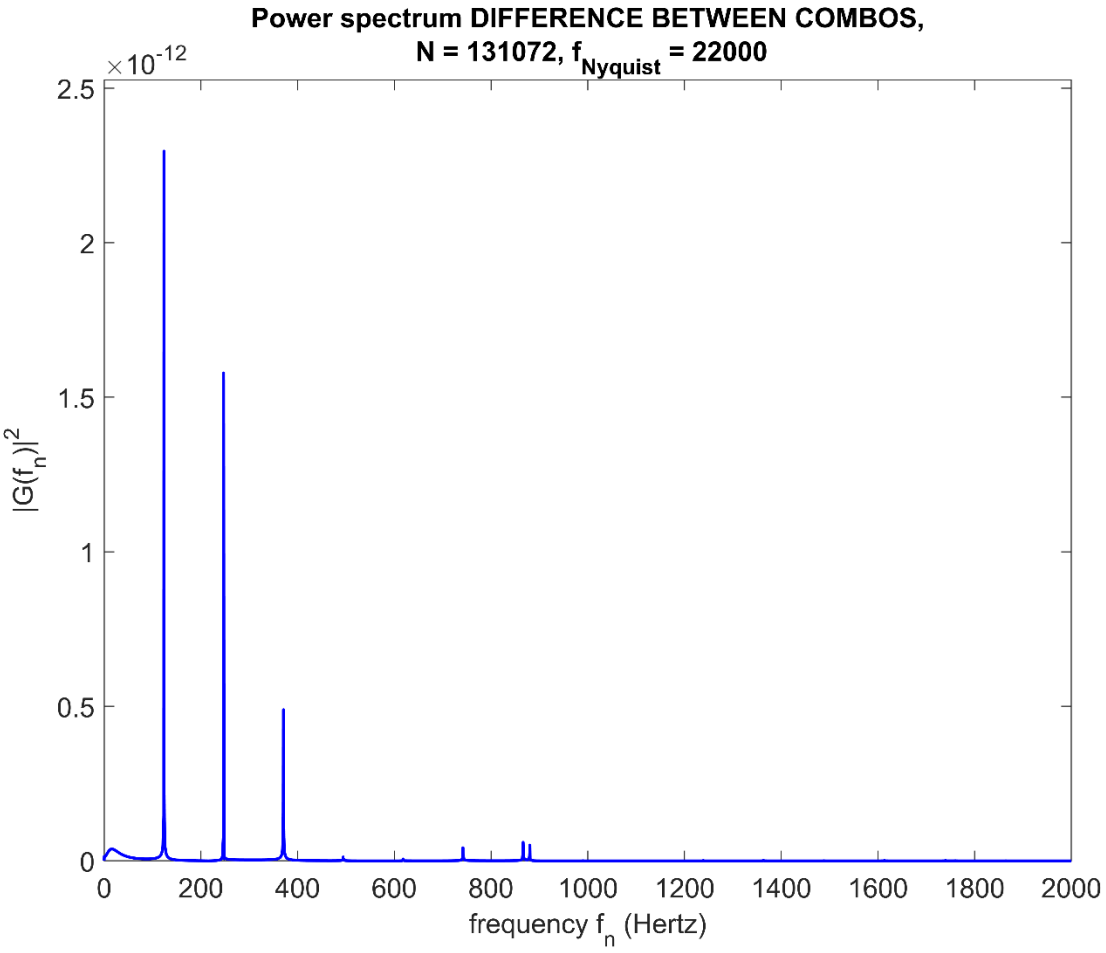

Figure 25: The absolute different of the power spectra of Figure 23 and Figure 24.

As in the case of the linear board model, the differences between the power spectra are small but significant. A comparison of Figure 19 for the linear model and Figure 25 for the non-linear model suggests that the non-linearity has little effect on the power spectra.

4.7 Non-linear Soundboard – Comparing Amplitudes

For the non-linear model, it is worthwhile to compare the displacements of notes played together and notes played separately and added later.

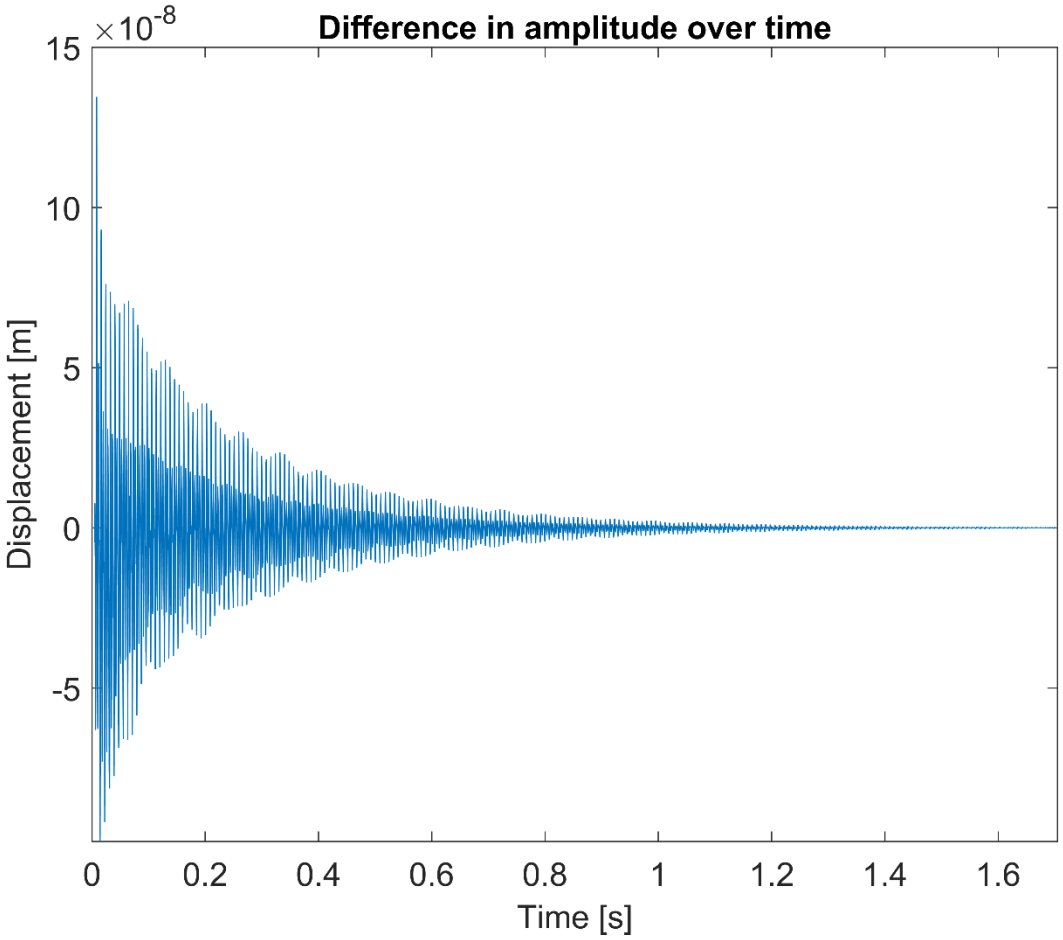

Figure 26: Displacement difference as a function of time at location 1. The graph shows the difference between the displacement when B2 and A5 are played together and when they are played separately and their displacements added.

Since the non-linear effects are small, we present in Figure 26 the difference between the displacements when B2 and A5 are played together and when they are played separately and added later. As before, the displacements are recorded at location 1 on the board. Figure 27 shows the power spectrum of this difference.

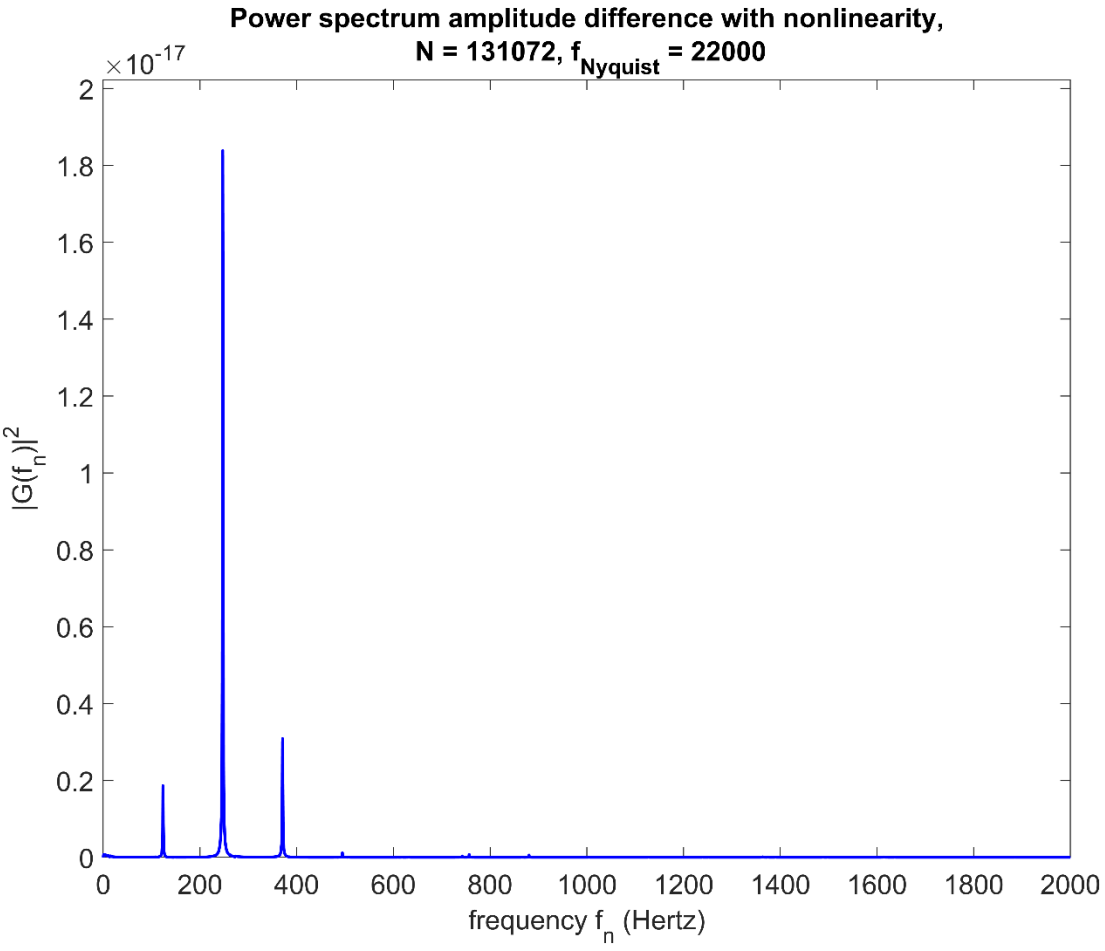

Figure 27: Power spectrum of the displacement as a function of time from Figure 26.

The data in Figure 26 and Figure 27 confirm that the non-linearity has a very small effect.

5 Summary & Conclusion

This work explored two scenarios of combining notes through computer simulations of a piano model. In the first, the two notes are played simultaneously and recorded, in the second, the notes are played separately, and their recorded signals added after the fact. Our piano model describes the soundboard, the strings, and the interaction between hammer and string. Using a finite difference method, we simulated the sound propagation of two notes, B2 and A5, being played separately and simultaneously. To investigate the difference between the scenarios, we determined power spectra for select locations on the soundboard and vibration patterns. To make the results relevant for real pianos within reasonable computational effort, we employ realistic parameters for materials while maintaining a simplified soundboard geometry. For most of the work, we used a linear soundboard model by Giordano. [4] As a first step toward a non-linear soundboard model, we investigated the effect of including one non-linear term in the partial differential equation for the board.

The input for the soundboard simulations are string forces generated in separate hammer-string simulations and applied to appropriate points on the bridge. Our simulation results for the string vibration show that the high-frequency note has lower amplitude vibrations that decay more rapidly than those of the lower note. The first soundboard simulations served to observe vibrations at different locations on the board. Our results allowed us to identify a location where both A5 and B2 have significant amplitudes. Soundboard simulations were evaluated at this location to generate data for displacements as a function of time and power spectra for separately played notes A5 and B2 and for the same notes played simultaneously.

The power spectra of the separate notes are representative of prerecorded notes and their sum represents notes as combined in a virtual instrument (scenario II). The power spectrum of the simultaneously played notes models the signal of scenario I. Comparing the two scenarios, we find measurable differences between the power spectra that might be perceptible to a trained ear.

To investigate the response of the whole soundboard, we generated vibration patterns for each note separately and played together. Our results show, as expected, a lower mode pattern for the lower frequency sound. We also find that the high amplitude vibrations are fairly localized so

that the signatures of both notes are evident in the vibration pattern when the notes are played together.

Finally, we explored the effect of a non-linear contribution to the partial differential equation describing soundboard vibrations. Our results show that the effect of this non-linearity on displacements and power spectra is very small.

6 Bibliography

[1] N. J. Giordano, Physics of the Piano, New York, NY: Oxford University, 2010.

[2] A. Chaigne and A. Askenfelt, "Numerical simulations of piano strings. II. Comparisons with measurements and systematic exploration of some hammer-string parameters," *J. Acoust. Soc. Am.,* vol. 95, p. 1631, 1994.

[3] A. Askenfelt and A. Chaigne, "Numerical simulations of piano strings. I. A physical model for a struck string using finite differences methods.," *J. Acoust. Soc. Am.,* vol. 95, p. 1112, 1994.

[4] N. J. Giordano, "Simple model of a piano soundboard," *J. Acoust. Soc. Am.,* vol. 102, no. 2, pp. 1159-1168, 1997.

[5] N. J. Giordano and M. Jiang, "Physical Modeling of the Piano," *EURASIP J. Applied Signal Processing,* vol. 7, pp. 926-933, 2004.

[6] R. Bogucki and S. Thomas, *Modeling and Simulation Final Project,* University of Akron, Dept. of Physics, Spring 2017.

[7] N. Giordano and H. Nakanishi, Computational Physics, Second Edition, Upper Saddle River, NJ: Pearson Education, Inc., 2006.

[8] H.-Y. Chia, "Nonlinear Analysis of Plates," New York, NY, McGraw-Hill Int., 1980, pp. 27-30.

[9] Howard Piano Industries, "Replacement grand piano Hammers," Howard Piano Industries, 2018. [Online]. Available: http://www.howardpianoindustries.com/replacement-grand-piano-hammers-individual/. [Accessed 12 April 2018].

[10] A. Stulov, "Physcial modelling of the piano string scale," *Applied Acoustics,* vol. 69, pp. 977-984, 2007.

[11] V. Bucur, Acoustics of Wood, Boca Raton, FL: CRC Press, 1995.